Determination of a Phospholipid Signature for Human Metabolic Syndrome Using Mass Spectrometry-Based Metabolomic Approaches

by

Rachel Kozlowski
B.Sc., McGill University, 2006

A Thesis Submitted in Partial Fulfillment
of the Requirements for the Degree of

MASTER OF SCIENCE

in the Department of Biochemistry and Microbiology

Determination of a Phospholipid Signature of Human Metabolic Syndrome Using Mass Spectrometry-Based Metabolomic Approaches

by

Rachel Kozlowski
B.Sc., McGill University, 2006

Supervisory Committee

Dr. Christoph H. Borchers, Supervisor
(Department of Biochemistry and Microbiology)

Dr. Caren C. Helbing, Departmental Member
(Department of Biochemistry and Microbiology)

Dr. Fraser Hof, Outside Member
(Department of Chemistry)

Supervisory Committee

Dr. Christoph H. Borchers, Supervisor
(Department of Biochemistry and Microbiology)
Dr. Caren C. Helbing, Departmental Member
(Department of Biochemistry and Microbiology)
Dr. Fraser Hof, Outside Member
(Department of Chemistry)

Abstract

Metabolic Syndrome (MetS) is an obesity-related disorder that predisposes an individual to several life-threatening diseases such as cardiovascular disease, hypertension and type 2 diabetes mellitus. The diagnosis of metabolic syndrome is based on the presence of at least 3 of the following 5 risk factors: elevated triglycerides, high blood pressure, high blood glucose, low HDL cholesterol and central adiposity. However, the biochemical mechanisms underlying the contribution of these irregularities are not fully understood. Currently, there is a need to better characterize MetS. Irregularity of lipid abundances, dyslipidemia, is known to be associated with MetS. However, little is known about the link between plasma phospholipids and human metabolic syndrome. In this study, mass spectrometry-based metabolomic approaches were employed using ultrahigh-resolution FTICR mass spectrometry to qualitatively analyze human plasma phospholipids and high-resolution QTOF mass spectrometry to quantitatively detect differences in the human plasma phospholipid profiles from 10 clinically-diagnosed metabolic syndrome patients and 8 lean healthy controls. The results point to the existence of a phospholipid signature of MetS. Five of the top twenty phospholipids contributing most to the difference in phospholipid abundance between the MetS and control group were identified using accurate mass-based database searching and MS/MS for structural confirmation. Relative differences in phospholipid abundances between MetS and controls for all top 20 phospholipids were shown to be statistically significant. These results may aid biomarker discovery and the accurate evaluation and prevention of diseases associated with dyslipidemia including human metabolic syndrome.

Table of Contents

List of Tables

List of Figures

Acknowledgments

I would like to take this opportunity to thank my supervisor, Dr. Christoph H. Borchers and Dr. Jun Han and for their dedication, support and guidance throughout this project; my committee members, Dr. Caren C. Helbing and Dr. Fraser Hof, whose guidance throughout this project was also much appreciated; Carol Parker for the countless hours she dedicated to the revision of this thesis; Dr. Sammy Chan for generously providing the metabolic syndrome samples as well as the healthy control samples; and the Department of Biochemistry and Microbiology for permission to conduct this research.

I would also like to thank my parents, Charlene Forget, Robert Kozlowski and Aneta Kozlowski for their ongoing support of my life goals as well as my best friend Nick Czernkovich for helping me laugh and realize what is important in life. I would also like to thank Martin Paine, whose love, patience and support has kept me focused through the cumbersome times of the writing process. I am grateful to each one of these generous individuals for helping shape the person I am today.

Chapter 1: Overview

1.1. Definition of Human Metabolic Syndrome

Human Metabolic Syndrome (MetS) is a cluster of metabolic abnormalities that occur together more often than expected by chance; these abnormalities predispose an individual to type II diabetes mellitus (T2DM) and cardiovascular disease (CVD).[1] According to the new International Diabetes Foundation (IDF) definition of MetS, which was used to diagnose patients in this study, in order for an individual to be diagnosed with metabolic syndrome, the following must be present: central obesity (waist circumference ≥ 94 cm for men of European descent and ≥ 80 cm for women with European descent (these values differ based on the ethnicity of the individual) plus at least 2 of the following: elevated triglyceride (TG) level (≥ 150 mg/dL (1.7 mmol/L)), reduced high density lipoprotein (HDL) cholesterol level (< 40 mg/dL (1.03 mmol/L)) for males and < 50 mg/dL (1.29 mmol/L) for females), elevated blood pressure (systolic BP ≥ 130 or diastolic BP ≥ 85 mm Hg) and/or elevated fasting plasma glucose (≥ 100 mg/dL (5.6 mmol/L)).[1] If an individual is currently being treated for one or more of these risk factors, it is presumed that the individual is positive for that risk factor.[1] Metabolic syndrome was first discovered by Gerald Reaven and has previously been known as Syndrome X, Reaven's Syndrome and/or insulin resistance syndrome.[2] Over the years, the definition has been modified, most notably with the inclusion of central obesity as a risk factor for the syndrome. However, there is disagreement between international health organizations concerning cutoff points for these risk factors; even the very inclusion of certain risk factors in the diagnostic criteria of MetS is disputed.[3]

1.2. Significance of Metabolic Syndrome and Related Diseases

1.2.1. Prevalence of Human Metabolic Syndrome

The need for improved molecular characterization of MetS must be stressed to enable a focus on prevention rather than treatment. Already, an overwhelming percentage of the world's population meet the criteria for MetS. A recent study of 1276 Canadians with an array of ethnic backgrounds found that while the prevalence of metabolic syndrome varies substantially between

ethnic groups, the overall prevalence of MetS was approximately 26%.[4] A 2002 study of 8814 participants over the age of 20 found the prevalence of MetS in the United States population to be approximately 24% as well.[5] Both of these studies used the definition of MetS as described by the Third Report of the National Cholesterol Education Program Expert Panel on Detection, Evaluation, and Treatment of High Blood Cholesterol in Adults (NCEP ATP III) criteria.[6] However, the impact of different definitions on the prevalence of MetS can be demonstrated by an Australian study of approximately 11,500 participants: all 3 definitions diagnosed approximately 15 – 21% of Australians with MetS, however, only 9.2% of the participants met MetS criteria of all three definitions.[5,6] As long as multiple definitions of MetS continue to exist, the prevalence of metabolic syndrome will be difficult to assess accurately. Comparison of MetS prevalence between populations using different MetS definitions will also be unreliable. The importance of using appropriate diagnostic criteria can be demonstrated by a recent study that compared 10-year mortality rates associated with different measures of obesity (body mass index (BMI), waist circumference and waist-to-hip ratio) among 359,387 participants from 9 European countries.[7] This study found that waist-to-hip ratio and waist circumference were better predictors of morbidity than BMI; in fact, for some low, healthy BMI values, an increase in waist circumference of only 5 cm represented a 17% increased risk of death.[7] However, unifying the definition of MetS is challenging as the mechanism of metabolic syndrome is also not well-understood. However, some progress is being made to elucidate the biochemical mechanisms involved in MetS. In recent years, many studies have examined the gene-environment interaction involved in MetS.[8-11] It is also already known that genes with possible implications in MetS can be modified by dietary and lifestyle habits (*e.g.*, alcohol dehydrogenase type 1C, apolipoprotein E, peroxisome proliferator-activated receptor-gamma, and the glutathione *S*-transferases T1 and M).[8] The development of a single worldwide definition of MetS is important to aid the early-detection and prevention of CVD and type 2 diabetes. Elucidation of the biochemical mechanisms involved in MetS will assist the realization of this objective. Once MetS can be earlier and more accurately diagnosed, appropriate treatments and preventive measures for this life-threatening syndrome can be more effectively developed.

1.2.2. Prevalence of Type II Diabetes Mellitus (T2DM)

It is estimated that 90% of T2DM can be attributed to excess weight.[12] Currently, over 1.7 billion adults worldwide are classified as overweight.[12] In Canada, the percentage of the population with diabetes is on the rise; in 1998, the diagnosed cases alone represented approximately 4.9 – 5.8% of the population ≥ 12 years of age.[13] While this percentage may seem inconsequential, the economic burden of diabetes-related complications in Canada in 1998 amounted to approximately $5 billion (USD).[13] In the United States, the direct and indirect costs of obesity in 2001 were estimated at $123 billion.[12] T2DM is also linked to CVD, in fact, coronary artery disease is the main cause of mortality in patients with type 2 diabetes.[14] In patients with type 2 diabetes, the presence of diseases related to fatty deposits in the arteries is 2 – 3 times higher than in individuals without diabetes.[14] T2DM is a costly yet potentially preventable disease.

1.2.3. Prevalence of Cardiovascular Disease (CVD)

In Canada, 33% of all deaths in 2003 were caused by CVD.[15] At a cost of $21.2 billion (CAD) in 1998, CVD represents the most costly Canadian disease.[16] In 2006, the American Heart Association estimated the annual cost of CVD in the USA to be $457.4 billion (CAD).[17] However, CVD is not isolated to the developed world. According to the World Health Organization, CVD is also a problem in low and middle-income countries where > 80% of all deaths due to CVD occur.[18] CVD is the leading cause of death globally.[18] It represents a costly but preventable worldwide problem. As such, it is important to define risk factors and detect these early so that CVD can be prevented before it poses serious health risks or causes death.

1.3.Human Metabolic Syndrome and Lipids in Blood

Dyslipidemia is an abnormality of lipid or lipoprotein concentrations in the blood.[19] In the clinic, the specific types of lipids involved in dyslipidemia as well as cut-off values for lipid concentrations deemed abnormal vary depending on the disease in question. These cut-off points also vary between major health organizations. As previously-mentioned, according to the NCEP ATP III, dyslipidemia involved in MetS is characterized by decreased HDL cholesterol and

increased triglycerides in plasma.[6] Despite inconsistent cut-off points, it is widely accepted that dyslipidemia is a major component of MetS.[20-23] Although the mechanisms of dyslipidemia are not well understood, recent progress in the scientific community has narrowed the gap in our understanding of dyslipidemia in MetS. The blood plasma (and serum) lipids of MetS patients have been studied in order to identify the specific lipid abundances that are abnormal in MetS-related dyslipidemia. Central obesity in MetS is associated with numerous alterations in plasma lipids and tissue lipid metabolism; in the liver, synthesis of very low-density lipoprotein (VLDL) and TG is increased and HDL synthesis is decreased.[23] When combined with decreased TG clearance by peripheral tissues, this leads to increased levels of plasma TG.[23] Phospholipids are a significant source of plasma fatty acids via pancreatic phospholipase A2 degradation of phospholipids to release free fatty acids and lysophospholipids. Differences in plasma fatty acid profile are also found to be associated with MetS: decreased n-6 and n-3 poly unsaturated fatty acids relative to saturated fatty acids and an increase in 16:1 (n-7) that was attributed to increased endogenous synthesis.[23] Another study suggested that the altered fatty acid profile of serum lipids in MetS (increased 14:0, 16:0, 16:1 (n-7), 18:1 (n-9), 18:3 (n-6) and 20:3 (n-6) and decreased 18:2 (n-6)) can be predicted by the activity of desaturases (enzymes involved in the introduction of double bonds at specific positions of long chain fatty acids and endogenous fatty acid synthesis).[22] Yet another study found increased levels of fatty acids corresponding to 16:0, 16:1, 18:1, 18:3 (n–6) and 20:3 (n–6) while levels of 18:2 (n–6) were found to be decreased in MetS patients.[24] These findings were attributed to the activity of Stearoyl-CoA desaturase-1 and Δ6-desaturase which were increased in MetS due to obesity while Δ5-desaturase activity decreased, which most likely plays an important role in MetS.[22] It is interesting that all of these fatty acid species are long chain fatty acids (LCFAs). LCFAs in the blood are thought to regulate appetite and glucose production by causing increased intracellular LCFA-CoA in the hypothalamus, therefore, alterations in this mechanism of homoeostasis may be related to central obesity and MetS.[24] Many studies have linked dyslipidemia in MetS with consumption of excessive amounts and/or poor quality dietary lipids and these studies have suggested that modification of dietary lipids may be important to modulating the risks associated with MetS.[20,21,24-26] In fact, a diet enriched in omega 3 phosphatidylcholine (PC (n-3)) was demonstrated to lower serum lipid levels and prevent or alleviate obesity-related disorders by suppressing fatty acid synthesis, increasing the serum adiponectin level and enhancing fatty acid

β-oxidation in obese rats.[27] In a Chinese population, phospholipid n-3 polyunsaturated fatty acids were also found to be significantly associated with lower risk of MetS and total fatty acid content was associated with greater risk of MetS.[28] While many studies have examined the total fatty acid content of human serum and/or plasma, little is known about the blood phospholipid levels in MetS patients as compared to healthy individuals. One study examined the serum HDL-phospholipid levels associated with MetS and CVD risk in Turkish adults.[29] Serum total phospholipid levels were found to be significantly higher overall in individuals with MetS or diabetes, and HDL-phospholipids were found to provide a protective effect from MetS and CVD.[29] Prior to the aforementioned study, neither serum total phospholipids nor HDL-phospholipids had been measured in epidemiologic studies.[29] However, the method used in the study that analyzed HDL-phospholipids was not comprehensive as it analyzed only choline-containing phospholipids. In addition, the study made no attempt to characterize the specific phospholipid species contributing to differences in either HDL-phospholipids or serum total phospholipids. Phospholipids are an important part of the human diet, they are known to play critical roles in inflammation response, cellular signaling and cholesterol transport.[30] The role of phospholipids in metabolic disorders and disease needs to be elucidated as previous research already suggests the possible implication of these species in obesity, type 2 diabetes mellitus and cardiovascular disease.

1.4.Human Phospholipids

1.4.1. Definition of Phospholipids

There are several major classes of phospholipids: phosphatidylcholine (PC), phosphatidylethanolamine (PE), phosphatidylinositol (PI), phosphatidylserine (PS) and sphingomyelin (SM). Additional phospholipid classes also include phosphatidic acid (PA), phosphatidylglycerol (PG) and ceramide phosphate (CerP). The chemical structures of the main phospholipid groups are shown in Figure 1. Phospholipids contain a hydrophilic head group, a glycerol backbone and one or two hydrophobic fatty acid tails. Phospholipids with a single fatty acid tail are also known as lysophospholipids. The fatty acid tail chemical composition is normally abbreviated as the number of carbon atoms followed by the number of double bonds, separated by a colon. Multiple fatty acid tails are separated by a forward slash. For instance, PC

(16:1/0:0) represents a lysophosphatidylcholine species containing a fatty acid tail 16 carbons long with a single double bond. A fatty acid with the first double bond located at the 3rd carbon in from the free end would be indicated by "n-3" while a fatty acid containing a double bond at the 6th carbon in from the free end would be indicated by "n-6" and so on.

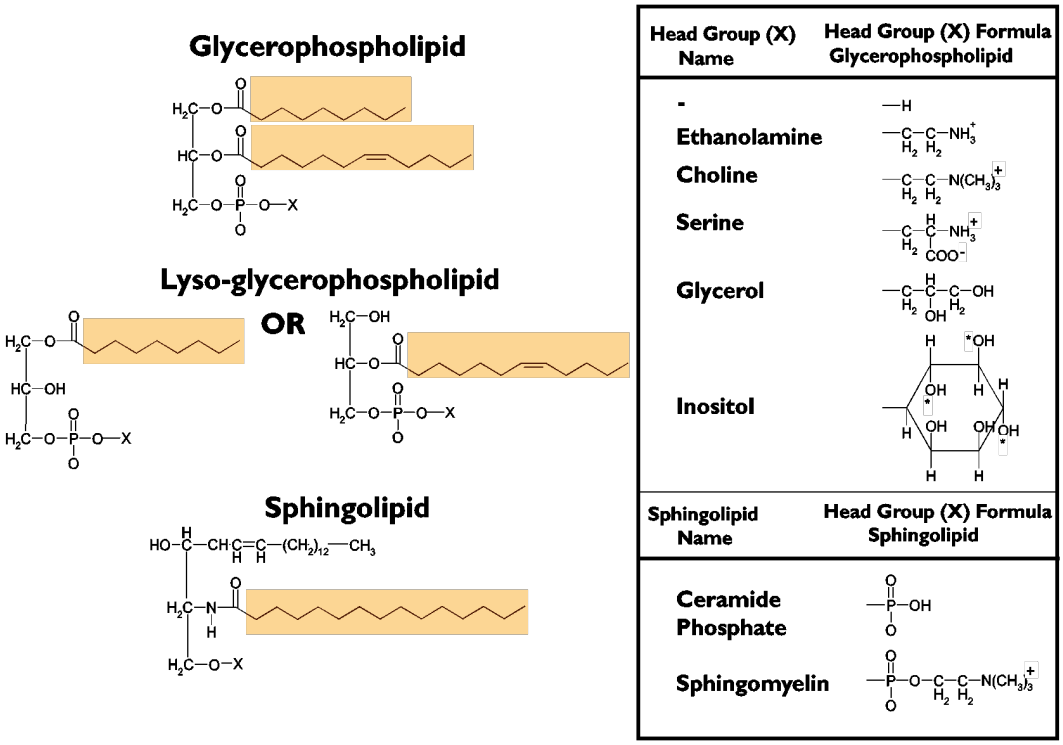

Figure 1. General Structures of Major Phospholipid Classes.
The structures of major phospholipid classes are shown. Phospholipids consist of a charged hydrophilic head group, a hydrophobic acyl chain tail and either a glycerol backbone (for glycerol phospholipids) or a sphingosine backbone (for sphingolipids). *Additional phosphate group(s) may be located on the hydroxyl moieties of the inositol head group.

1.4.2. Biochemical Significance of Phospholipids

Because phospholipids have both a hydrophobic tail region and a hydrophilic head region, the physiological function of a phospholipid may be due to either one or both of these regions. Phospholipids are a key component of cell membranes and are important in nutritional and signal transduction for the maintenance and metabolic regulation of living cells.[21] Apart from being the basic structural elements of cell membranes and the outer layer of plasma lipoproteins, phospholipids can serve as ligands for receptors, enzyme substrates for lipoprotein

metabolism, second messengers in signal transduction, precursors of essential biomolecules, intracellular traffickers of cholesterol as well as modulators of the immune system.[31, 32] In studies in rats and rabbits, PC has been associated with protective effects on liver and cholesterol-lowering properties have been reported; PC also enhanced secretion of bile cholesterol, and reduced lymphatic cholesterol absorption and hepatic fatty acid synthesis.[33-35] Phosphatidylinositol, a less abundant component, was shown to increase levels of HDL-cholesterol in rabbits and humans.[36,37] In addition, a cholesterol-lowering effect of PE as well as its base, ethanolamine, has been reported in rats where this was attributed to increased excretion of neutral steroids in fecal matter.[38,39] Many studies have examined the functions of *cellular* phospholipids, but very limited information exists about the physiological functions of *dietary* phospholipids.[21]

1.4.3. Phospholipid Synthesis and Transport

Dietary fat is comprised primarily of TG but also contains approximately 10% phospholipid content, which is predominantly phosphatidylcholine (PC) and phosphatidylethanolamine (PE).[21] Dietary fat is broken down into fatty acids and other components which are then absorbed through the intestinal wall of the small intestine. These metabolized components are then converted into TG and incorporated along with cholesteryl esters into the interior of chylomicrons which are coated by an exterior layer of apolipoproteins, phospholipids and cholesterol.[30] The chylomicron then transports these lipids through the lymphatic system, bloodstream and into tissues.[30] Activated by apoC-II in capillaries, lipoprotein lipase releases fatty acids for cellular entry where they are oxidized for use as an energy source or re-esterified for storage.[30] The chylomicron remnants then travel through the blood and are taken up by endocytosis in the liver; any excess fatty acids are converted to TG and packaged with apolipoproteins into VLDL. These are then transported through the bloodstream for delivery to muscle and adipose tissue.[30] Removal of lipids causes the VLDL to become LDL which is taken up by extrahepatic tissues from which extra cholesterol is transported back to the liver as HDL.[30] This depleted HDL is then free to extract lipids from circulating chylomicron and VLDL remnants.[30] Thus, exogenous lipids from the diet are primarily transported as chylomicrons and endogenous lipids are primarily transported as VLDL, LDL and HDL.

However, because HDL is able to extract lipids from chylomicrons and endogenous lipids will eventually include exogenous lipids, it is difficult to completely separate the two sources.

In human blood, phospholipids are also a major component of the membranes of erythrocytes, white blood cells and platelets. Erythrocytes also contain a significant amount of cholesterol associated with phospholipids that is strongly bound to haemoglobin within the erythrocyte itself.[40] While the mechanism is not well-known, these haemoglobin-bound phospholipids and cholesterol contributes to lipid efflux from erythrocytes into plasma.[40] Also, human phospholipid transfer protein (PLTP) transfers phospholipids from lipoproteins rich in TG to HDL during lipolysis.[41] Due to the exchange of phospholipids within components of human plasma, it is perhaps more accurate to examine whole plasma phospholipid composition rather than only one or several individual components when examining plasma phospholipid abundance and/or composition.

1.5.Metabolomics and Mass spectrometry

1.5.1. Metabolomics

Metabolomics involves the qualitative and quantitative analysis of all of the small molecule compounds (metabolites) present within a biological system. Metabolites represent the end-point products of biochemical processes from multiple metabolic pathways and are the closest to and most predictive of a "metabolic phenotype".[42] The study of these metabolites and their respective abundances can be used to make inferences about complex biochemical processes. Two key complementary approaches used to investigate metabolites are metabolic profiling and metabolic fingerprinting. Metabolic profiling is an investigation of a specific group of known metabolites relating to a specific metabolic pathway or present in a specific biological tissue/sample of interest. Metabolic fingerprinting instead looks to compare patterns of both known and unknown metabolites, "fingerprints", which change in response to perturbations, such as disease or environmental factors. Detection and identification of specific metabolites that show concentration changes in response to these perturbations can provide insight into the biochemical mechanisms underlying disease development and progression. Metabolic fingerprinting can also be used as a diagnostic tool, by comparing an individual's metabolic fingerprint to those of healthy and diseased subjects to determine the presence of a disease.[42] The

effectiveness of treatment strategies may also be studied through monitoring the shift of a metabolic fingerprint back to one resembling a healthy state.[42]

Mass spectrometry and nuclear magnetic resonance (NMR) are two of the most widely used tools in the field of metabolomics. These techniques are somewhat complementary.[43,44] While the use of NMR for metabolomic analysis allows for recovery of the analyte after analysis and is very reproducible, mass spectrometry is both very sensitive and specific.[43]

1.5.2. Mass spectrometry (MS)

Among various analytical technologies currently used in metabolomics, including NMR, high detection-sensitivity of mass spectrometry (MS) renders it a crucial tool for comprehensive measurement of metabolites in complex biological samples.[44] In fact, recent improvements to liquid chromatography coupled to mass spectrometry (LC/MS) (*e.g.*, ultrahigh performance liquid chromatography MS, or UPLC/MS) have broadened the applicability of MS-based metabolomics.[45]

Mass spectrometry is a powerful analytical tool. It can be used to accurately determine the molecular masses of thousands of compounds of interest from data acquired in a single experiment. In addition, it can provide quantitative information about an analyte at extremely high sensitivity (*i.e.*, sub-attomole range). Mass spectrometry can also be useful for detailed structural analysis of a compound of interest using ion fragmentation techniques. These qualities make mass spectrometry a powerful tool for studying low-abundance compounds (*e.g.*, some species of plasma phospholipids) for which both qualitative and quantitative information is needed.

Generally, a mass spectrometer consists of an ionization source, an analyzer and a detector. The sample, containing ionizable analytes, is injected into the ionization source. These analytes are converted into the gas phase and detected in either positive or negative ion mode. The mass analyzer separates these ions by mass-to-charge ratio (*m/z*), and transfers them to the detector. The mass analyzer may also contain a collision cell where the analyte precursor ions can be fragmented into product ions in order to provide information about the structure of the analytes. This is termed tandem mass spectrometry, MS/MS, or MS^2. These ion fragments are then allowed to pass through a second mass analyzer where they are separated. Signals from the

detector are transformed into a final interpretable mass spectrum, visualized using specialized software programs.

The ionization technique used in this experiment was electrospray ionization (ESI). ESI uses a small, highly-charged metal capillary through which a volatile solvent containing the analyte is forced and, because the droplets are highly charged, forms a fine spray. After formation of the aerosol, the volatile solvent begins to evaporate, which forces the dissolved analyte ions closer together. This generates strong repulsive forces that drive the ions apart in a process termed Coulombic fission. The combination of Coulombic fission and solvent evaporation produces dehydrated ions, which are then directed into the mass analyzer (shown in Figure 2).[46] ESI is considered a "soft" ionization method because it results in less fragmentation of the analyte than other ionization techniques.

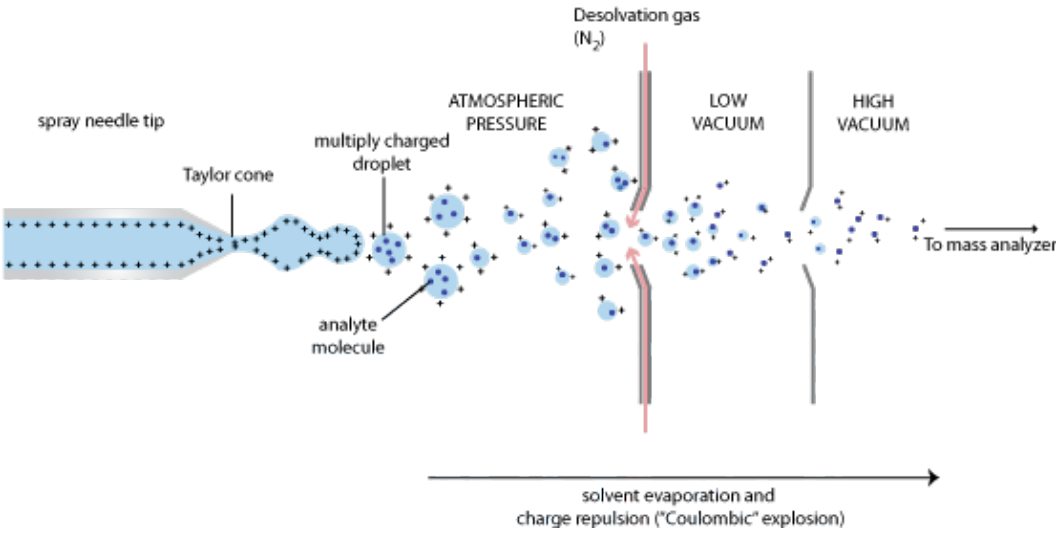

Figure 2. Electrospray Ionization Mechanism.[47]
Charged analytes in solution enter the source of the mass spectrometer as multiply charged droplets. Through a combination of Coulombic fission and solvent evaporation, analytes enter the gaseous phase for downstream detection by the detector of the mass spectrometer.

Two commonly-used mass analyzers include the time-of-flight (TOF) and the quadrupole. In a TOF analyzer, ions are accelerated into a field-free region until they strike the detector. As suggested by the name, time-of-flight, the amount of time that the ion takes to strike the detector is directly proportional to the mass of the ion.[48-50] Another popular mass analyzer is

the quadrupole (shown in Figure 3). A quadrupole mass analyzer consists of four parallel rods that emit RF (radio frequency) and DC (direct current) voltages to guide the ions. Unwanted ions can be destabilized in order to avoid detection, while ions of interest are stabilized and permitted to pass through the quadrupole and travel towards the detector. Setting these voltages to a fixed value or scanning these voltages allows selective or non-selective transmission of ions respectively.[51,52] This is in contrast to a TOF, which does not scan and detects all sample ions.

Two mass spectrometry instruments were used in this study. One is a high-resolution orthogonal quadrupole-time-of-flight (QTOF) mass spectrometer; the other is a hybrid quadrupole-Fourier transform ion cyclotron resonance (FTICR) mass spectrometer, which will be described in the next paragraph. A QTOF mass spectrometer, as implied by the name, is a hybrid instrument consisting of a quadrupole mass analyzer and a TOF analyzer. A schematic diagram of the QTOF MS instrument used in this study is shown in Figure 4.

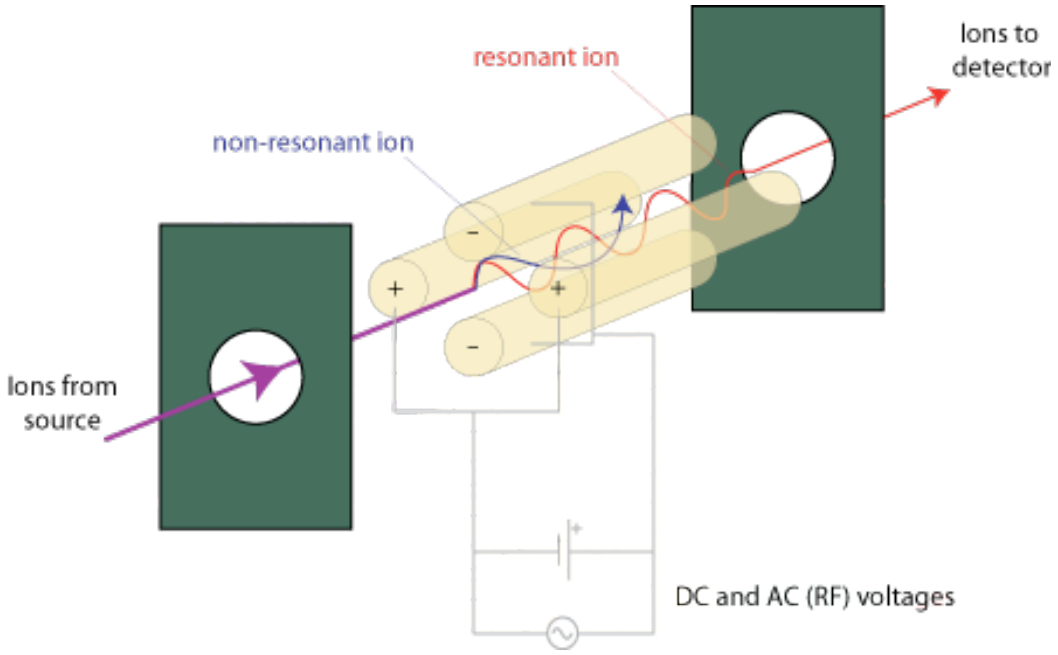

Figure 3. Quadrupole Mass Analyzer.[47]
Using a combination of direct current and radio frequency voltages, ions can be filtered so that only ions of interest (resonant ions) are selected in the quadrupole for downstream detection while other ions (non-resonant ions) are destabilized to ensure that they do not reach the detector.

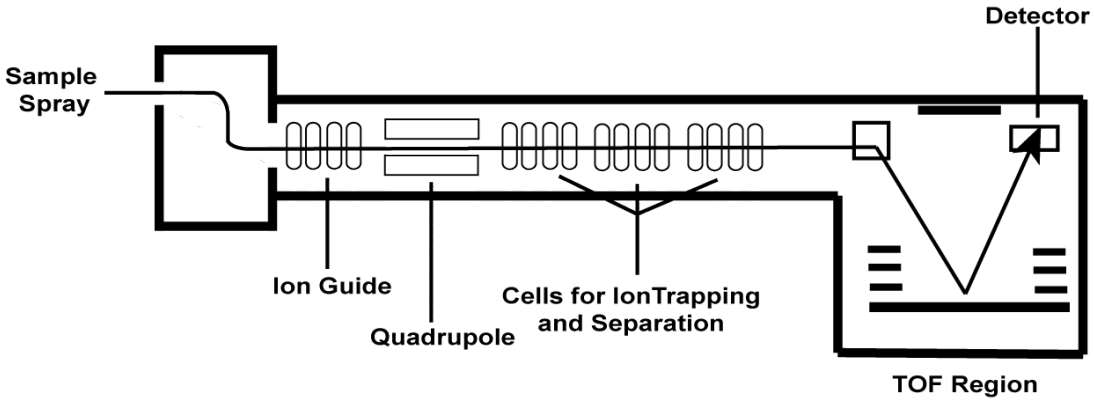

Figure 4. Schematic Diagram of the QTOF Mass Spectrometer.
Ions enter the mass spectrometer at the source. They then travel through the mass spectrometer to the quadrupole mass analyzer for filtering. After leaving the quadrupole mass analyzer, reach the TOF analyzer where they are reflected by an electrostatic mirror (reflectron) for increased mass resolution upon detection.

Most modern mass spectrometers contain detectors that generate an electronic signal from the collision of the incident ion beam on a resistive conductive surface.[53] For example, an electron multiplier (EM) device uses a process called secondary electron emission to amplify the signal from the original ions.[54] This is the way in which ions are detected in the QTOF mass spectrometer. The FTICR MS is significantly different from other types of mass spectrometry in that mass analyzer of an FTICR MS instrument is an ion cyclotron resonance (ICR) cell, which is wrapped with a superconducting magnet. Figure 5 shows the typical configuration of an ICR cell. A basic FTICR sequence is composed of 5 consecutive events: ion quenching, injection, trapping, excitation and detection. In the ICR cell, the analytes are under the influence of the magnetic field. The orientation of the magnetic field in conjunction with excitation RF pulses (*chirps*) cause the analytes to move in cyclotron orbits proportional to their individual mass-to-charge ratios. In this case, instead of hitting a resistive conductive surface of an electron multiplier, as is the case for some other mass spectrometers, ions with the same m/z will pass by the detector at its unique cyclotron frequency for detection.[55] For ions that pass by, an image current is generated and this ion image current will decay with time following ion excitation. The sum of all of these currents makes up a convoluted free induction decay (FID) signal.[56,57] This FID signal is de-convoluted by applying a mathematical operation called Fourier transform. As a result, the time-domain FID signal is converted into a composite frequency-domain signal. After calibration with standard compounds of known m/z, the frequency-domain signal is further

converted to the mass-to-charge signal, which is finally represented as a mass spectrum.[57] This process is demonstrated in Figure 5.

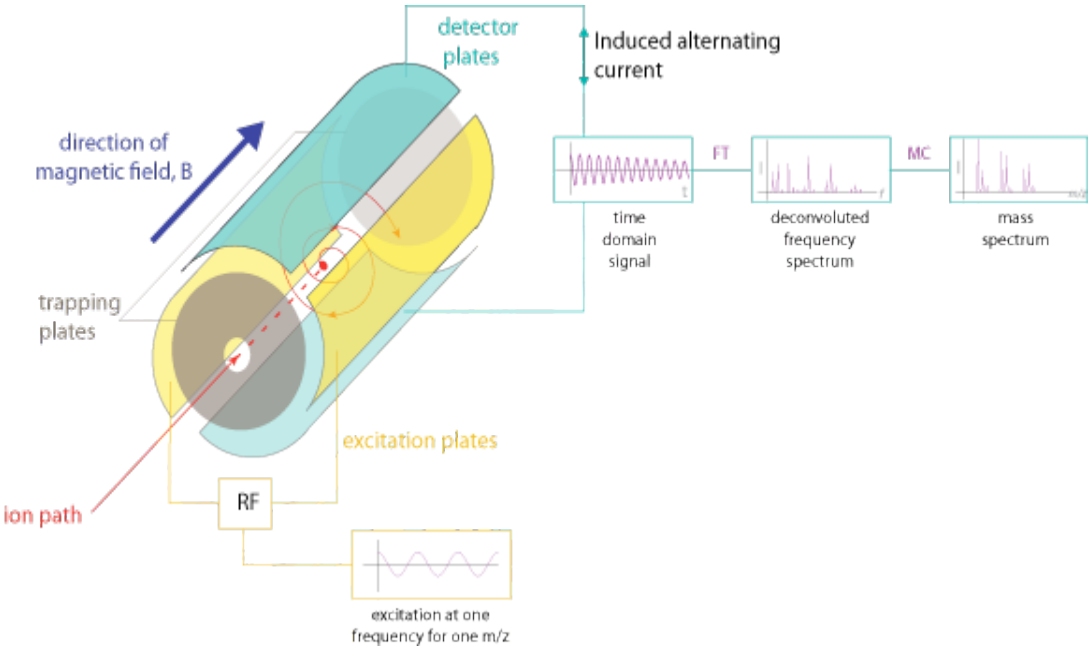

Figure 5. Mechanism of Ion Trapping, Excitation and Detection in the ICR Cell.[47] Ions enter the ICR cell and, under the influence of RF pulses and a magnetic field, move in cyclotron orbits proportional to their m/z values. The sum of all image currents induced by ions passing by the detector plates creates a FID signal (time domain signal). This is then de-convoluted by a Fourier transformation into a composite frequency spectrum, and then finally into an interpretable mass spectrum**.**

The most significant feature of the FTICR mass spectrometer is its ultrahigh mass resolution and mass accuracy, which result from the extremely accurate measurement of the ion cyclotron frequency of an ion under the stable superconducting magnetic field. In this study, we used a 12-Tesla ultrahigh-resolution hybrid quadrupole-FTICR MS instrument (Figure 6) for molecular profiling of human plasma phospholipids. Using the 12-Tesla FTICR MS instrument, a mass resolution of up to 1,000 000 can be achieved when narrowband detection mode is used. Sub-ppm mass accuracy can be routinely obtained for the simultaneous detection of hundreds to thousands of components in a complex mixture, without sacrificing its ultrahigh mass resolution.

Within the FTICR mass spectrometer used in this study, the analyte ions generated by an external ESI source travel through a series of ion guides (lenses and other optics), two quadrupoles (one pre-quadrupole and one mass filter quadrupole) , a hexapole and ion transfer optics before they reach the ICR cell for trapping, excitation and detection. MS/MS fragmentation using collision-induced dissociation (CID) was performed in the hexapole. This hexapole acts as a collision cell to fragment the precursor ions of an analyte, selected by the front-end quadrupole mass filter, into product ions by applying a biased voltage on the hexapole. Mass spectral interpretation of the product ion m/z values can provide important information about the chemical structure of the analyte.

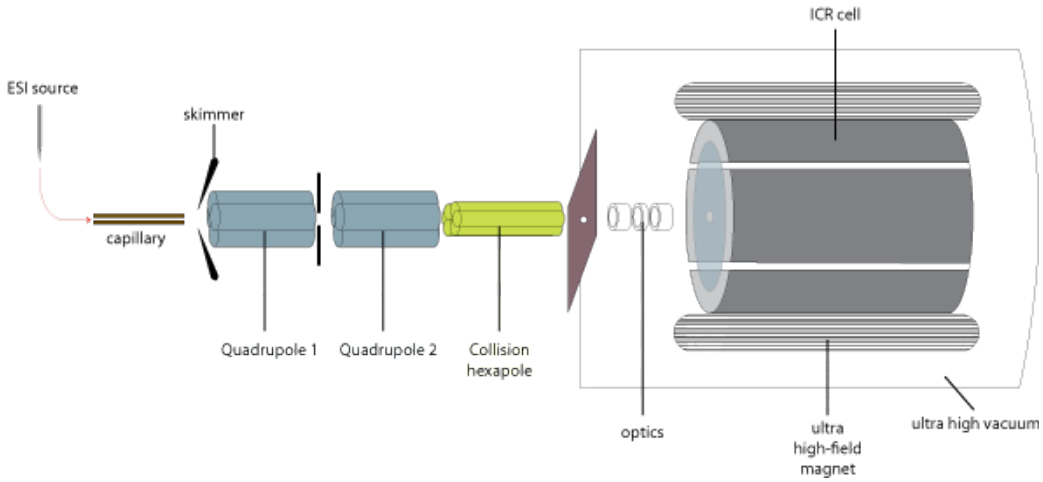

Figure 6. A Hybrid Quadrupole-FTICR Mass Spectrometer.[47]
This instrument consists of a combination of quadrupoles to guide ions of interest, a hexapole which can be used for MS/MS fragmentation and ion optics to transfer ions into the ICR cell, where, under the influence of an ultra high-field magnet, ions will be detected.

1.5.3. Lipid Metabolome Database: LIPID MAPS

In this study, one of the most comprehensive lipid metabolome databases, LIPID MAPS[58], was used to assign the phospholipids detected in this study. LIPID MAPS (LIPID Metabolites And Pathways Strategy) is a consortium created in 2003 with the aim of comprehensively quantitating and identifying all of the lipid species in mammalian cells as well as their changes in response to perturbation.[58] This is a multi-institutional effort involving six core lipidomics laboratories specializing in the extraction, identification and quantitation of glycerolipids, fatty acyls, glycerophospholipids, sphingolipids, sterols and prenols.[58] Other key laboratories involved in this consortium contribute to LIPID MAPS with knowledge from their

respective specialized fields of lipid oxidation, lipid synthesis, mass spectrometric imaging, macrophage biology, genomics and bioinformatics.[58] The lipid structures found in the LIPID MAPS database are obtained from five main sources: the core laboratories and partners of the LIPID MAPS Consortium, lipids identified by LIPID MAPS experiments, computationally-generated structures for appropriate lipid classes, manually-curated, novel lipids submitted to peer-reviewed journals and biologically relevant lipids obtained from LIPID BANK, LIPIDAT and other public sources.[59, 60] The LIPID MAPS database contains 22,500 unique lipid structures (including 1960 glycerophospholipids and 3909 sphingolipids) as of April 21st 2010, rendering it the largest public lipid database in the world.[60]

1.6.Study Hypothesis

Dyslipidemia is widely accepted as being associated with MetS and previously-conducted research suggests a possible role of phospholipids in lipid metabolism. As mentioned previously, recent research also suggests a possible role of phospholipids in MetS, T2DM and CVD. However, a comprehensive analysis of human plasma phospholipids on the molecular level has not yet been conducted to attempt to distinguish MetS from healthy controls. This study is based on the hypothesis that there is a detectable difference in the abundance of human plasma phospholipids in metabolic syndrome patients as compared to healthy controls; the identification of the species contributing to these differences will reveal a plasma phospholipid signature of human metabolic syndrome.

If there is, in fact, a detectable difference in specific human plasma phospholipid species, this research could aid in the determination of the biochemical mechanism by which MetS occurs. It is important to examine all lipid components in human plasma, including phospholipids, especially because links to irregularities in lipoprotein metabolism and MetS, T2DM and/or CVD have already been made. Without studying human plasma phospholipids, the mechanism of lipoprotein metabolism in healthy individuals vs. MetS patients may remain incomplete. Elucidation of the complete biochemical mechanism of lipid irregularity in MetS may aid the development of effective treatments for MetS and the implementation of appropriate preventative measures for the prevention of MetS, T2DM and CVD.

It is also difficult to compare MetS prevalence in different populations within a nation or internationally without a unified definition of MetS. This then complicates the accurate assessment of possible genetic and/or environmental factors that may be involved in MetS. The implementation of effective preventative measures and treatments for MetS is also made difficult. An examination of differential human plasma phospholipid abundances in MetS patients *vs.* healthy controls may aid our understanding of the biochemical mechanisms of the syndrome and assist with the development of an accurate definition of MetS. Appropriate measures can then be taken to more accurately detect and prevent metabolic syndrome and its related life-threatening diseases such as type II diabetes and CVD.

This study employed mass spectrometry-based metabolomic approaches, including the use of ultrahigh-resolution FTICR MS for molecular profiling of human plasma phospholipids and the use of UPLC coupled to high-resolution QTOF mass spectrometry to quantitatively detect the differences in human plasma phospholipid abundance in a small cohort of clinically-diagnosed metabolic syndrome patients and lean healthy controls. This was done in order to reveal a phospholipid signature of MetS. A general schematic of the methodology and experimental design is shown in Figure 7.

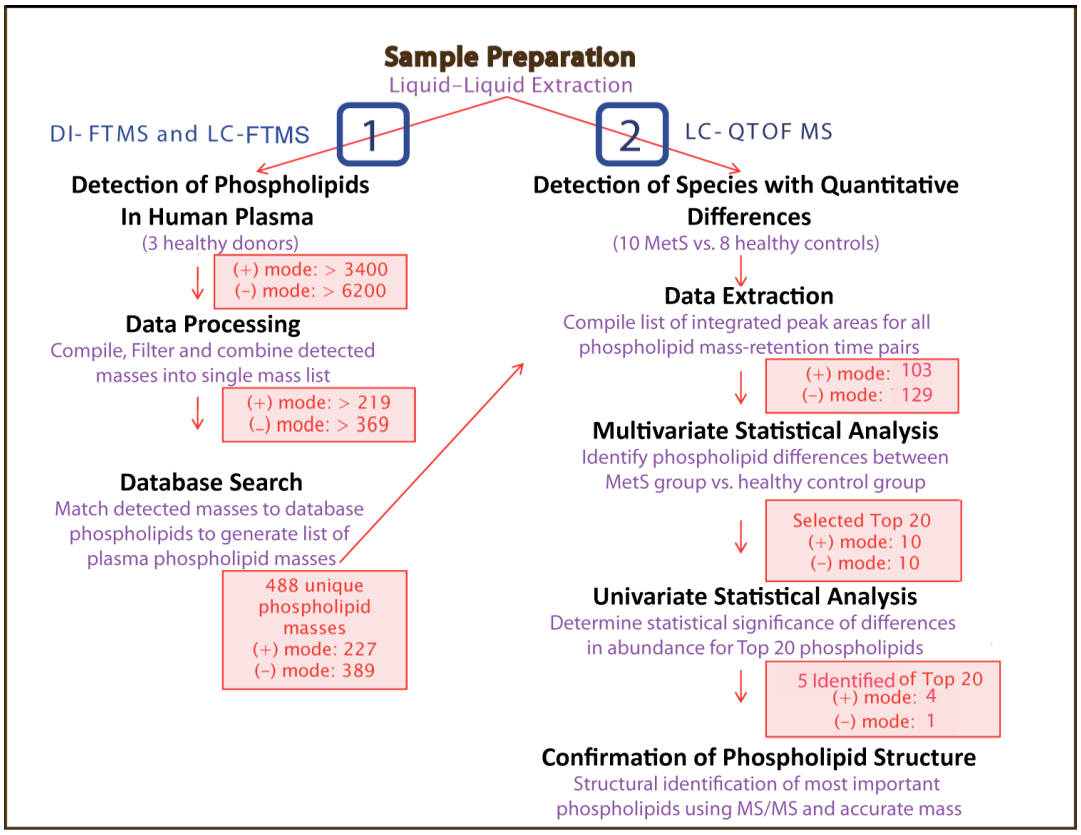

Figure 7. General Schematic of Experimental Methodology.
FTICR MS was used for profiling of human plasma phospholipids. The phospholipid mass list obtained from the profiling experiment was then used for mass-directed data extraction of UPLC/QTOF MS data for relative quantitation of plasma phospholipids in MetS samples *vs.* lean healthy control samples.

Direct infusion (DI) and LC were used in conjunction with FTICR MS to comprehensively profile the phospholipids found in human plasma. After these phospholipids were identified using accurate masses to search the LIPID MAPS database, a final mass list was generated for targeted quantitation of these species by UPLC/QTOF MS. Phospholipids were extracted from 10 MetS patients and 8 healthy controls and analyzed using UPLC/QTOF MS. Metabolite features were extracted from the LC/MS profiles using a targeted approach based on the m/z values of the database-matched phospholipid masses. The extracted metabolite features were saved as two-dimensional data matrices in a format amenable to subsequent multivariate analysis in order to detect a statistical difference in phospholipid abundance between the MetS group and healthy control group. The top 20 phospholipids contributing most to this statistical

difference in phospholipid abundance between the MetS and control groups were subjected to univariate statistics; this was done to determine whether the difference between groups could be attributed to specific phospholipid species at a statistically significant level of confidence. Structural confirmation of these top 20 phospholipids was then attempted by combining offline UPLC fractionation with subsequent DI/FTICR MS/MS on UPLC fractions of interest.

Chapter 2: Molecular Profiling of Human Plasma Phospholipids by FTICR MS-Based Metabolomics

2.1.Introduction

As previously mentioned, phospholipids are an important class of human lipids. They are biologically functional, playing key roles in cholesterol transport, cellular signalling, inflammation response as well as being precursors to other biologically important metabolites. Over the past decade, mass spectrometry-based metabolomic techniques have been used to successfully profile an array of metabolites in biological tissues and fluids.[61-63] In fact, mass spectrometric analysis has already been applied to a number of studies relating to diabetes and CVD.[64-66] It is important that human plasma phospholipids are profiled and structurally characterized so that changes in these species due to pathogenesis, such as those involved in MetS, may be more accurately assessed. In this chapter, ultrahigh resolution FTICR MS was employed, in combination with DI and LC, for comprehensive characterization of phospholipid profiles in human plasma.

2.2.Materials and Methods

2.2.1. Sample Collection

Three human plasma samples collected from 3 healthy donors (38-year-old male, 47-year-old female and 59-year-old female) were purchased from Innovative Research (Novi, Michigan, USA). All donors were negative for both diabetes and CVD. These plasma samples were treated with Na_2 EDTA to prevent clotting and had been stored at -20 ^{o}C according to the accompanying sample information sheet. Upon receipt, each plasma sample was stored at -80 ^{o}C until required for experimental analysis. Human plasma samples were divided into 1 mL aliquots immediately after the first thaw. All human plasma samples used for profiling experiments underwent no more than 2 freeze-thaw cycles.

2.2.2. Extraction of total phospholipids

The total plasma lipid was extracted with liquid-liquid extraction (LLE) using a modified Bligh and Dyer procedure.[67] Briefly, in a 1.5-mL Eppendorf tube, a 50-µL aliquot of each plasma sample was added with 50 µL H_2O, 450 µL of $CHCl_3$/MeOH (1:2, v/v) and 2 grains of butylated hydroxytoluene (BHT) as a lipid antioxidant. After vortex mixing and brief sonication for 3 x 10 s in an ice-water bath, the tube was placed at -20 ^oC for 1 hour to precipitate as much protein as possible. The tube was then centrifuged for 15 min at 13,000 rpm and 4 ^oC in a bench top micro-centrifuge. The supernatant was transferred to a new tube and 600 µL of $CHCl_3$/MeOH (1:2, v/v) was added to the residual pellet. The pellet was completely suspended by vortex mixing and the sample was then extracted again using the same conditions described above. The supernatant was combined with the previously-collected supernatant and 200 µL of H_2O was added. After vortex mixing, the tube was centrifuged again for 5 min at 13,000 rpm to separate the solution into two phases. The lower ($CHCl_3$-containing) organic phase was carefully collected and transferred into a new tube. The upper aqueous layer was extracted additional 2 times with 300 µL of $CHCl_3$, and the lower ($CHCl_3$) phases were removed and combined with the previously-collected organic phase. The pooled organic phase was then dried using a Thermo Savant SpeedVac system (Thermo Fisher Scientific Inc., Waltham, MA, USA). The dried residue was then reconstituted in 100 µL isopropanol (IPA) and stored overnight at -80 ^oC for mass spectrometric analysis the following day.

2.2.3. DI/FTICR MS

For DI/FTICR MS experiments, 20 µL aliquots of IPA-dissolved samples were further diluted with 50 µL IPA and 30 µL H_2O immediately prior to mass spectrometric analysis. A predefined amount of the standard "ESI Tuning Mix" solution (Agilent Technologies, Santa Clara, CA, USA) was spiked into each sample as reference standards, to a final dilution in solution/ sample of 1:200, for internal mass calibration. Formic acid (FA) was added to yield a final concentration of 0.1% (v/v) for analysis in positive ESI mode or 0.01% (v/v) for analysis in negative ESI mode. These samples were then directly infused into a Bruker Daltonics Apex-Qe 12-Tesla hybrid quadrupole-FTICR mass spectrometer. The instrument was tuned and calibrated across an *m/z* range of 250 to 1100 Th for both ionization modes. The sample was infused at a

flow rate of 2 µL/min using a KD Scientific syringe pump (KD Scientific Inc., Holliston, MA, USA). Survey scan mass spectra were acquired using a broadband detection mode until a total of 500 scans were reached. The following parameters were used for all DI/FTICR MS analyses: ESI voltage: 3600~3900 volts; collision cell gas (Ar) flow: 0.3 L/min; source temperature: 180 ^{o}C; drying gas (N_2) flow: 3.5 L/min; nebulising gas (N_2) flow: 2 L/min; FID transient size: 1,024 kilobytes per second.

2.2.4. LC/FTICR MS

For LC/MS, the following values were used for all LC/FTICR MS analyses: ESI voltage: 3600-3900 V; collision cell gas flow: 0.3 L/min; source temperature: 180 ^{o}C; drying gas flow: 3.5 L/min; nebulising gas (N_2) flow: 4 L/min; free induction decay (FID) transient size: 512 kilobytes per second. An Ultimate 3000 HPLC system (Dionex Corporation, Bannockburn, IL, USA) coupled to the FTICR MS instrument and a BEH C-8 column (1 mm I.D. x 50mm, 1.7 µm particle size, Waters Corporation, Milford, MA, USA) were used.

The organic mobile phase consisted of LC/MS-grade acetonitrile (ACN) (Sigma-Aldrich, St. Louis, MO, USA) containing 0.1% (v/v) FA for analysis in positive ESI mode or 0.01% (v/v) in negative ESI mode. The aqueous mobile phase consisted of H_2O (Sigma-Aldrich, St. Louis, MO, USA) with an identical concentration of FA to that used in the organic mobile phase for each ionization mode. Sample vials were kept at 5 ^{o}C during LC runs in order to minimize sample degradation. The column was maintained at 40 ^{o}C.

Prior to LC/MS analysis, the column was equilibrated using a minimum of 2 blank gradient runs at a flow rate of 60 µL/min. After optimization for best chromatographic resolution and peak shape, 10 µL of each sample was injected onto the column. The gradient began at a 10% organic mobile phase and then linearly increased to 100% organic mobile phase over a duration of 85 minutes. This was followed by a five-minute wash-step using 100% organic mobile phase. After this, a column-equilibrium step ran for 10-minutes using 10% organic mobile phase. This equated to an overall LC/MS run time of 100 minutes per sample injection. This gradient was used for all 3 plasma samples.

2.2.5. Data Processing

2.2.5.1. DI/FTICR MS Raw Data

The recorded DI/FTMS datasets were batch-processed using a custom-written VBA script embedded in the Bruker's *DataAnalysis*® software package. This VBA script enabled post-acquisition internal mass calibration with the reference masses of the standard "ESI Tuning Mix" solution, spectral charge deconvolution and monoisotopic peak recognition based on the calculated isotopic distribution patterns for elements of C and Cl, and monoisotopic peak selection for all ions detected with signal-to-noise ratio (S/N) ≥ 3. Next, this script wrote the extracted monoisotopic masses from each spectrum to a tab-delimited text file that contained the corresponding values for *m/z*, charge state, neutral mass, intensity and S/N value. The batch text files were then imported into custom-developed *NI LabView*® software, *1D-PAMD,* for salt adduct analysis and peak alignment across all 3 samples. A salt adduct was recognized if the mass difference between any two experimental masses matched the theoretically-calculated mass difference for $[M+H]^+$ *vs.* $[M+Na]^+$ or $[M+K]^+$ in positive ESI mode or for $[M-H]^-$ *vs.* $[M+Cl]^-$ in negative ion mode within 3 ppm. The masses of Na and K used for positive ion salt adduct calculations were 22.9892 Da and 38.9632 Da, respectively, and the mass of Cl used for negative ion salt adduct calculations was 34.9694 Da. After this salt adduct determination, only those masses corresponding to $[M+H]^+$ and $[M-H]^-$ were kept. These values were combined across all samples for positive and negative ionization modes, respectively. The resultant monoisotopic masses were saved as a peak text file and imported to the LIPID MAPS database to search for mass-matched phospholipids. The glycerophospholipid and sphingolipid sections of the LIPID MAPS database were used for this accurate mass-based matching. The searches were performed using a batch mode, and within a mass window of +/- 0.0005 Da, which is equivalent to +/- 5ppm for a 1000-Da species.

2.2.5.2. LC/FTICR MS Raw Data

LC/MS data files were processed using the "Molecular Features" peak-finding algorithm within the Bruker *DataAnalysis*® software suite to extract all of the species in the individual LC/MS profiles detected in each ion mode with an S/N cut-off value of 3. The extracted

metabolite features, including the values for the monoisotopic *m/z*, S/N and peak area were exported into Microsoft Excel and saved as a text file. One text file per LC/MS profile was saved in a format amenable to processing with the *1D-PAMD* software. Salt-adduct analysis and peak alignment were subsequently conducted using a similar strategy to that outlined in the above "2.2.5.1. DI/FTMS Raw Data" section, except that the allowable mass error was 6 ppm, instead of 3 ppm. As described previously, salt adducts were recognized based on the theoretical mass difference for the Na and K adducts in positive ion mode and for the Cl adduct in negative ion mode. The larger allowable mass error was selected due to software limitations, which did not allow for internal calibration (post data acquisition) for LC/MS data files acquired in this experiment. After salt-adduct analysis, inter-sample alignment was conducted using the same mass error of 6 ppm and the resultant aligned monoisotopic masses from all of the combined LC/MS data were saved as a text file and used to search against the LIPID MAPS database for possible glycerophospholipids and sphingolipids. This was done using the batch search mode of LIPID MAPS, but with a mass error tolerance of +/-0.001 Da, equivalent to +/-10 ppm for a 1000-Da species.

2.2.5.3. Data Alignment and Combining

All the unique neutral phospholipid masses from both direct infusion MS datasets and both LC/MS datasets were then combined into one mass list. The phospholipid mass values returned from the LIPID MAPS database searches were used to create a final phospholipid mass list. After the exact mass error (ppm) was calculated for each database mass, duplicate mass values were deleted using the "Excel Unique and Duplicate Data Remove Software" add-in (Sobolsoft, http://www.sobolsoft.com). When duplicates were found, the smallest associated value for mass error was saved along with its corresponding neutral mass. The resultant final list of unique phospholipid masses along with their mass-matched phospholipids was generated and later used for mass-directed data extraction of UPLC/QTOF MS data files for determination of the quantitative differences in phospholipid abundance between MetS samples and healthy controls.

2.3. Results and Discussion

2.3.1. Sample preparation and extraction

Previously-conducted experiments have demonstrated that changes in the chemical composition of plasma compounds may be found at detectable levels after as few as 10 freeze-thaw cycles.[68-70] Therefore, in order to maintain the fidelity of the metabolic profile in each plasma sample, all of the plasma samples were stored at -80 ^{o}C upon receipt and were subjected to as few freeze-thaw cycles as possible. Also, all the samples were kept on ice or 4 ^{o}C during the entire sample preparation process in order to maintain sample integrity. This was done to minimize metabolite degradation as well as other chemical changes to metabolites. In addition, BHT, a commonly used antioxidant, was added to the plasma samples prior to metabolite extraction to minimize the risk of oxidation of plasma phospholipids during the process of sample preparation and MS analysis.

2.3.2. DI/FTICR MS *vs.* LC/FTICR MS

Direct infusion (DI) is a chromatography-free approach that introduces a liquid sample directly into the ionization source of a mass spectrometer. DI is simple, quick and inexpensive compared to other sample introduction methods. Therefore, DI is a particularly attractive tool for high-throughput MS detection of a large number of metabolites without tedious front-end chromatography. Direct infusion, combined with the ultrahigh-mass accuracy FTICR MS (which can be used to identify species based on accurate mass measurement alone) was used for molecular profiling of human plasma phospholipids in this study.

Due to the sample complexity of plasma samples and the large biological variability of humans, however, LC/MS is better suited for comprehensive analyte detection. Isomers that cannot be resolved using DI may be separated based on their differing retention times using LC. LC/MS separates a complex mixture of analytes by connecting an on-line LC column in front of the entrance of the ESI source of the mass spectrometer. In liquid chromatography, analytes interact with the column stationary phase and can be selectively retained based on their physical and chemical properties (such as hydrophobicity). These analytes can be sequentially eluted from the column based on the differences in these physical and chemical properties. Due to this additional separation, LC reduces one of the major problems of ESI when analyzing a highly

complex mixture: the ionization suppression or enhancement of ionized analytes due to the presence of other ions. This is because LC reduces the number of compounds present in the source at the same time, thus reducing the ionization suppression/enhancement effects that are associated with ESI. This phenomenon, known as the ESI matrix effect, is particularly problematic for low-abundance analytes when highly abundant species are entering the ESI source simultaneously.

FTICR MS provides the highest mass resolution of all current mass spectrometric techniques. With the 12-Tesla FTICR mass spectrometer, sub-ppm mass accuracy can be routinely obtained if the instrument is appropriately calibrated with internal mass calibrants. This makes it possible to identify at least hundreds of metabolites in a complex biological sample without the need for time-consuming upfront chromatographic separation. Identification can be achieved by querying the available metabolome databases using the measured accurate molecular masses, or by using the rational chemical formulas generated from these masses, in combination with some limitations of elemental compositions, electron configurations and other chemical rules.[70] In this study, samples were analyzed by FTICR MS in order to ensure that the masses of the detected species were as accurate as possible. In this way, a very large number of unique phospholipid masses could be accurately measured while at the same time a search of the LIPID MAPS database could assign phospholipids based solely on their accurate masses. A range of 250 – 1100 Th was used for mass spectral acquisitions because a brief survey of the LIPID MAPS database, the most comprehensive database currently available for human and other mammalian lipids, revealed that only <5 phospholipids species fall outside this mass range. For DI/FTICR MS, a total of 500 scans were accumulated to average a mass spectrum in order to detect weakly-ionizing or low-abundance phospholipids.

For LC/FTICR MS experiments, formic acid used to ionize species in both positive and negative ion modes, but at different concentrations, in order to maintain good peak shape as well as high ionization efficiency across both ionization modes.[72] A UPLC C-8 column was used instead of an HPLC column or C-18 column because peak shapes were improved when the column was used.

2.3.3. Data Processing

2.3.3.1. DI/FTICR MS and LC/FTICR MS Raw Data

For salt analysis, only the most common salt adducts (Na, K, Cl) were considered for removal in DI/MS and LC/MS experiments in order to minimize the risk that potentially important phospholipid species were incorrectly assigned to these salt adducts (and subsequently removed). The allowable mass error for DI/FTMS datasets was 3 ppm while the mass error tolerance for salt adduct analysis and data alignment across multiple LC/MS runs were 6ppm. This mass error for LC/MS datasets is larger because, as mentioned previously, the vendor-specific software could not handle batch post-acquisition internal mass calibration, and manual internal mass calibration across each analyte peak of an LC/MS profile is impractical. Another factor that accounts for the larger mass error is that the space-charge effects in the ICR cell change with time during an LC/MS run, in that the number of ions that enter the ICR cell is different at different times. The space-charge effect is the major source of mass error for FTICR MS. Therefore, the masses detected by LC/MS were less accurate than those detected by DI/FTICR MS.

2.3.3.2. Data Alignment and Combining

In both ionization modes combined, FTICR MS experiments detected more than 3400 metabolite features in positive ion mode and over 6200 in negative ion mode after peak alignment and salt adduct discrimination analysis. After database searching against LIPID MAPS, 369 masses matched at least one phospholipid mass belonging to either the glycerophospholipid or sphingolipid class, within 6 ppm, using data acquired using LC/FTICR MS in negative ion mode. Using LC/FTICR MS data acquired in the positive ion mode, 219 masses returned one or more hits from LIPID MAPS with mass errors within 6 ppm. For direct infusion MS data acquired in negative ion mode, 88 masses matched phospholipid masses in the LIPID MAPS database within a mass error of 2 ppm. For data acquired in positive ion mode, DI/FTICR MS data returned 73 matches to unique phospholipid masses within 2 ppm after searching LIPID MAPS.

The two Venn diagrams in the lower half of Figure 9 display the number of unique and overlapping phospholipid masses between LC and DI for both ionization modes. In positive ion

mode, LC/MS detected almost 20 times as many unique (non-overlapping) species than were detected using DI/MS. In negative ion mode, LC/MS detected almost 10 times as many non-overlapping phospholipid masses than detected using DI/MS. However, it is also important to note that although LC/MS was able to detect many more phospholipid masses than were detected by DI/MS, DI was still able to detect some species that LC did not. These two Venn diagrams clearly show the benefit of LC/MS over DI/MS while highlighting the complementary nature of LC/MS and DI/MS. After these 4 lists of phospholipid masses from LIPID MAPS databases were combined and duplicates were removed, a total of 488 unique phospholipid masses with associated mass errors < 6 ppm were obtained (227 of these were detected in positive ion mode and 389 in negative ion mode). Figure 9 also displays the number of unique and overlapping phospholipid masses between each ionization mode. As shown in the Venn diagram located in the upper portion of Figure 9, detection in both negative and positive ion modes are complementary. Also, we see that a large number of species are preferentially detected in negative ion mode over positive ion mode. The mass error associated with the final matched phospholipid list was notable. Approximately 65% of the matched phospholipid masses on the list had associated mass errors below 3 ppm. In addition, over 72% of these phospholipid masses matched two or more phospholipid isomers in the LIPID MAPS database.

Although more than 3400 and 6200 metabolite features were detected in positive and negative ion modes respectively, many of these peaks did not match any phospholipid masses in the database. This was suspected to be mainly due to the presence of other metabolites such as neutral lipids, steroids, unidentified phospholipids, etc., or even those from unexpected fragmentation products of these metabolites. In fact, this seemed to be the case as less than 10% of the positive-ion peaks detected matched phospholipid masses from the database. It was expected that a larger number of phospholipids would be detected in negative ion mode because it is known that phospholipid ions generated for the majority of phospholipid classes are preferentially ionized in negative ESI mode. In fact, this was also the case as, for this entire study, a larger number of peaks were always detected in negative ionization mode as compared to positive ionization mode.

For decades, the phospholipids of individual components of blood have been studied in depth, including erythrocytes, fibroblasts, lymphocytes, neutrophils and platelets.[73-75] However, as previously mentioned, the study of total phospholipid content in blood may have advantages

over the study of the phospholipid content of a single component, most notably because of the dynamic exchange of phospholipids between components of human blood. The comprehensive analysis of human plasma phospholipids conducted in this current study is a step towards accomplishing this goal. A study that used DI/MS by triple quadrupole-linear ion trap mass spectrometry identified 50 different phospholipids in whole blood.[76] Another study conducted an analysis of phospholipids in negative ionization mode and identified over 100 phospholipids using ion-trap mass spectrometry (MS^2 and MS^3).[77] However, the identification of 100 phospholipids is not indicative of a comprehensive analysis in comparison to the 488 unique phospholipid masses detected in this current study. Also, as seen in Figure 8, detection of phospholipids in only the negative ion mode is far from comprehensive. It should be noted that the detection of species matching 488 unique phospholipid masses is the largest number of unique human plasma phospholipid masses identified in a single experiment. In addition, a significant number of monoisotopic masses detected by FTICR MS did not match masses in the LIPID MAPS database. A cursory analysis of the mass defects and isotopic distributions of these unidentified masses revealed at least several good candidates for previously-uncharacterized plasma phospholipids. The resulting mass list and associated mass error is summarized in Appendix A.

In order to provide information about the distribution of phospholipid classes found in human plasma, all phospholipid masses of this mass list were categorized into 9 classes based on the phospholipid head group to which each mass matched. These categories were ceramide phosphate (CerP), phosphatidic acid (PA), phosphatidylcholine (PC), either phosphatidylcholine or phosphatidylethanolamine (PC/PE), phosphatidylethanolamine (PE), phosphatidylglyceride (PG), phosphatidylinositol (PI – including PIP), phosphatidylserine (PS) and sphingomyelin (SM). A visual representation of this intra-group phospholipid class composition as a percentage of the total 488 matched phospholipid masses is shown in Figure 8. This intra-group comparison of phospholipid class composition is also shown numerically in column 1 of Table 1.

As shown in Table 1, comparison of the phospholipid numbers among the 9 phospholipid classes assigned from the 488 unique masses revealed that the largest number of phospholipids detected in human plasma by MS were PS, PC and PE (including the PC/PE group) while the lowest number of phospholipids detected were in the categories of SM and CerP. It is important to note that these numbers may not correlate with absolute concentration in plasma. Instead,

these numbers are more of an indicator of phospholipid class variability in plasma, as this phospholipid composition is based on the number of *different* phospholipids detected per phospholipid class. In addition, without further structural analysis of these database-matched and unmatched phospholipids, we cannot determine the exact order of relative variation within phospholipid classes with a high degree of certainty. Therefore, while this analysis of phospholipid class distribution may provide some insight into variation of human plasma phospholipids within each phospholipid class, it is by no means exact.

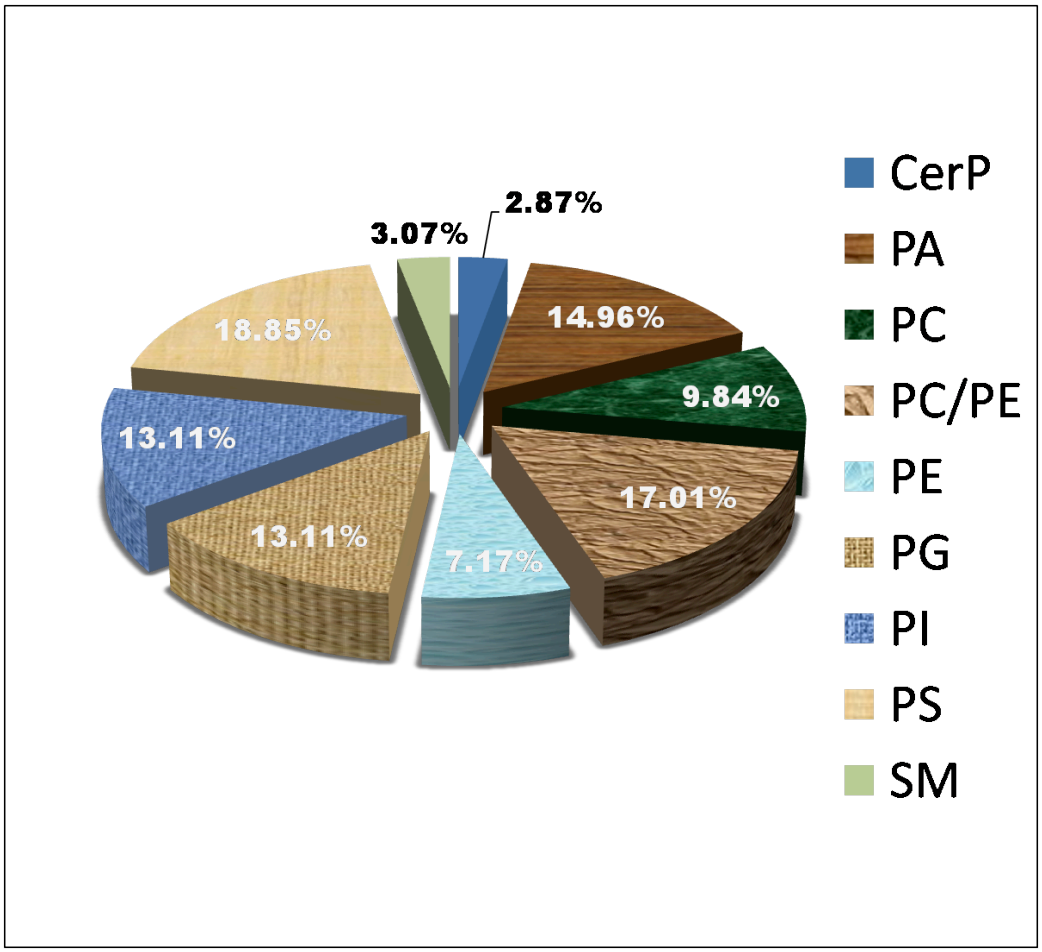

Figure 8. Phospholipid Composition of Matched Masses Detected Using FTICR MS. Pie chart showing the phospholipid class composition, as expressed by percentage, of all database-matched phospholipid masses detected by FTICR MS.

Table 1. Distribution of Phospholipid Classes Based on LIPID MAPS Database Searching.
Phospholipid masses detected at specific stages of this study were separated into their respective phospholipid classes. Percentage of total phospholipids quantitated was obtained by dividing the number of integrated unique phospholipid masses by the number of total unique phospholipid masses in each phospholipid class. This ratio was then expressed as a percentage.

Phospholipid Class	Number of Phospholipid Masses Detected (by FTICR MS)	Number of Phospholipid Masses Quantitated (by QTOF MS)	Top 20 Quantitated Phospholipid Masses	Percentage of Phospholipid Masses Detected by FTICR MS Quantitated
Ceramide Phosphate (CerP)	14	0	0	0.00
Phosphatidic Acid (PA)	73	15	3	20.55
Phosphatidylcholine (PC)	48	32	5	66.67
Phosphatidylcholine or Phosphatidylethanolamine (PC/PE)	83	67	8	80.72
Phosphatidylethanolamine (PE)	35	24	1	68.57
Phosphatidylglycerol (PG)	64	17	1	26.56
Phosphatidylinositol (PI)	64	6	0	9.38
Phosphatidylserine (PS)	92	47	2	51.09
Sphingomyelin (SM)	15	12	0	80.00
Total Phospholipid	488	220	20	45.08

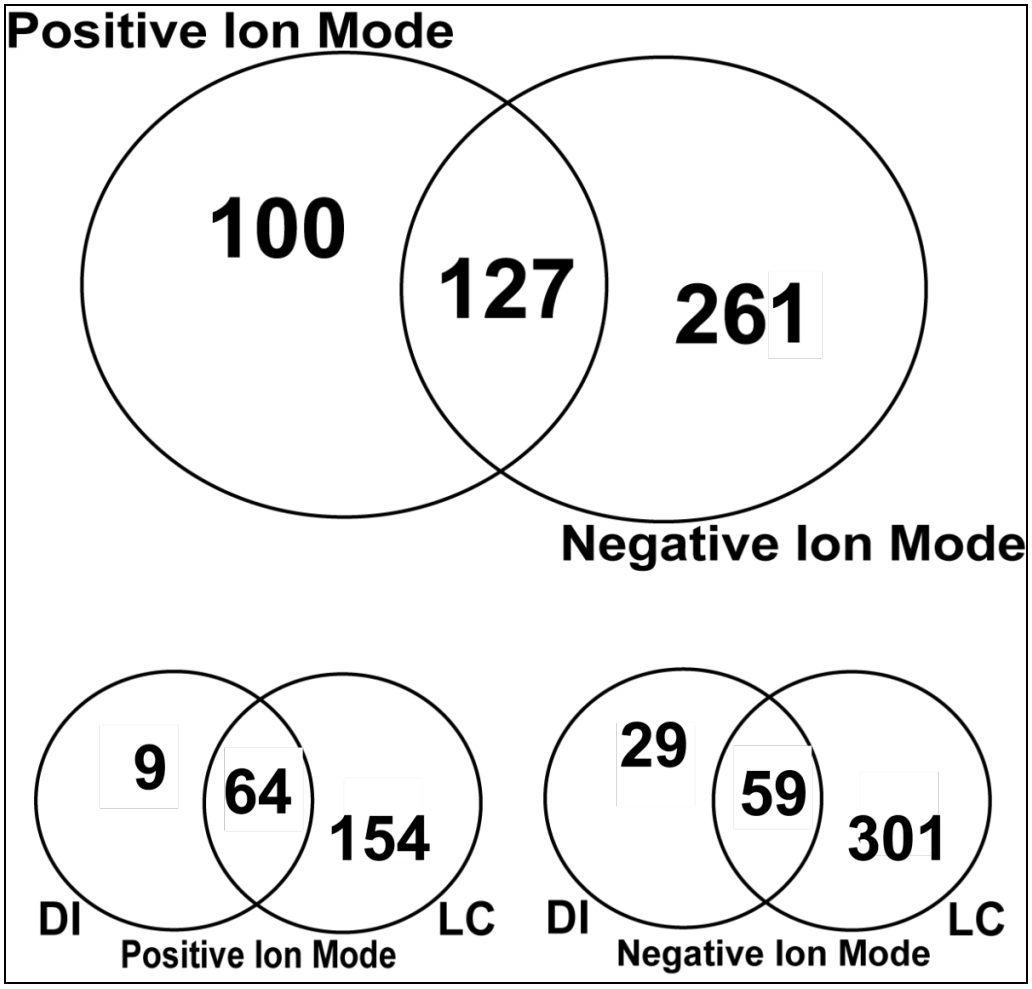

Figure 9. Overlap of Matched Phospholipid Masses Detected by FTICR MS.
Venn diagrams showing the distribution of matched phospholipid masses detected in negative ion mode and positive ion mode overall (one uppermost Venn diagram) and using DI and LC coupled with FTICR MS for each ion mode (two lowermost Venn diagrams).

2.4.Summary

The ultrahigh mass accuracy of the FTICR mass spectrometer allowed for accurate-mass based identification of 488 unique human plasma phospholipid masses after searching the LIPID MAPS database. The classes containing the largest number of phospholipids in human plasma were found to be PC, PE and PS. DI/FTICR MS and LC/FTICR MS are powerful, complementary techniques for the profiling of phospholipids in human plasma. The power of direct infusion, in this case, lies in the fact that hundreds of scans can be accumulated in a single

spectra so that low abundance species are more likely to be detected using this technique as compared to liquid chromatography. The power of liquid chromatography, here, lies in the fact that it reduces ion suppression/enhancement effects so that a larger variety of analytes are more likely to be ionized as compared to direct infusion. Both positive and negative ion mode were also complimentary as some phospholipids were expected to ionize more efficiently in positive ion mode while others were expected to ionize more efficiently in negative ion mode.

Chapter 3. Determination of a Phospholipid Signature of Human Metabolic syndrome in Plasma

3.1.Introduction

Due to the previously mentioned biological importance of phospholipids in humans, it is important to study the changes in these species in response to disease, as these changes may help elucidate the biochemical mechanisms of these diseases. Because phospholipids make up a significant percentage of the human diet, irregularities in phospholipid abundances may be particularly useful for determining the mechanism of pathogenic states of metabolism, including MetS. Metabolic fingerprinting is a useful tool for the detection of changes in abundances of metabolites that may be related to specific biological processes, drug treatment effects, or disease states. Mass spectrometry-based metabolomics is already being used to study the possible role of phospholipids in type 2 diabetes patients.[64] In this current study, UPLC was coupled to QTOF MS for relative quantitation of differences in human plasma phospholipids in MetS patients *vs.* lean, healthy controls. Offline UPLC fractionation was combined with DI/FTMS and MS/MS to characterize the structure of the phospholipids contributing most to the statistically significant differences in phospholipid abundance between the MetS group and lean healthy controls.

3.2.Materials and Methods

3.2.1. Human Plasma Samples

A cohort of 18 human plasma samples collected from 10 clinically-diagnosed metabolic syndrome patients and 8 lean healthy donors (controls) were used in this experiment to detect relative differences in phospholipid abundance between MetS and healthy controls. The presence of MetS was assessed using the new International Diabetes Federation (IDF) definition of the metabolic syndrome.[1] These samples were generously supplied by Dr. Sammy Chan, the medical director of the BC Metabolic Syndrome Program, from the Division of Cardiology at St. Paul's Hospital in Vancouver, BC. All samples were stored at -80 ^{o}C upon receipt. Age and gender information pertaining to the donors of these clinical plasma samples is shown in Table 2.

Table 2. Human Plasma Sample Information for Clinical Cohort.
Plasma sample identifiers (1-18) as well as the gender, the age and sample group assignment of individuals included in the cohort of samples used for QTOF MS quantitation are shown in the table below. Equal numbers of males and females aged 34 through 65 participated in this study.

Plasma ID	Gender	Age	Sample group
01	M	50	Metabolic Syndrome
02	M	47	Metabolic Syndrome
03	M	34	Metabolic Syndrome
04	M	42	Metabolic Syndrome
05	M	44	Metabolic Syndrome
06	F	37	Metabolic Syndrome
07	F	45	Metabolic Syndrome
08	F	50	Metabolic Syndrome
09	F	59	Metabolic Syndrome
10	F	47	Metabolic Syndrome
11	M	49	Lean control
12	M	65	Lean control
13	F	45	Lean control
14	F	47	Lean control
15	F	57	Lean control
16	M	38	Lean control
17	M	34	Lean control
18	F	35	Lean control

3.2.2. Sample Preparation

All 18 samples were extracted using the same LLE protocol used for the phospholipid profiling experiments described in Chapter 2, except that only 25 µL of each plasma sample was used as the starting material for extraction. Therefore, all volumes reported in the LLE protocol were halved, and the extracted phospholipids were diluted to IPA/H_2O (50:50, v/v) immediately before LC/MS analysis.

3.2.3. UPLC/QTOF MS

For LC/QTOF MS experiments, a Waters Acquity UPLC system was coupled on-line to a Waters Synapt HDMS (QTOF) mass spectrometer. The UPLC column used was a Waters BEH C-8 column, 1mm I.D. x 50 cm, 1.7 μm particle size. Binary solvent gradient elution was carried out to chromatograph the plasma lipids and both (+) and (-) ion modes were employed for MS detection. The mobile phases used were: aqueous (A) 0.1% FA for positive ESI mode or 0.01% FA for negative ESI mode; organic (B) LC/MS-grade IPA/ACN (2:1, v/v) (containing 0.1% or 0.01% FA. Low concentrations of other additives (triethyl amine, phosphoric acid, ammonium bicarbonate) were also evaluated during method development with the aim of improving peak shapes and chromatographic resolution. FA was found to provide the best performance for this study. Samples were kept at 5^{o}C in the autosampler and the column was maintained at 45^{o}C for the duration of the LC/MS analyses. Prior to running each set of samples, 3 blank gradient runs were used to pre-equilibrate the column. To maintain consistent high mass accuracy, a lock-mass spray of leucine enkephalin (m/z: 556.277 in (+) ESI mode; m/z: 554.262 in (-) ESI mode) at a concentration of 50 pg/μL was used. The calibration was carried out using the lock-mass data acquired from an average of 3 continuous scans, 0.15 s per scan for every 10 seconds. The parameter settings for QTOF MS were as follows: ESI voltage 3.0 kV for (+) ESI and -2.5 kV for (-) ESI; sampling cone voltage 45 V; source temperature 110 ^{o}C; desolvation gas (nitrogen) flow rate 500 L/hour; desolvation gas temperature 350 ^{o}C; scan rate 0.25 s/scan. A mass detection range of 250 to 1100 Th was used for both positive and negative ionization modes, and the mass spectrometer was tuned and calibrated over this same mass range immediately prior to sample runs. Using a LC flow rate of 80 μL/min., 10 μL of each sample was injected and the mobile phase gradient began at an initial composition of 40% B, and then increased linearly to 100% B over 30 minutes. The mobile phase was maintained at 100% B for another 5 minutes. The column was then re-equilibrated for 3 minutes with 40% B between every two LC/MS runs, leading to a total run time of 38 minutes per LC/MS run.

3.2.4. Data processing

QuanLynx, the platform-specific quantitation software included in the Waters MassLynx software suite, was used to conduct targeted, mass-directed data extraction. To do this, the

theoretical monoisotopic $[M+H]^+$ values for positive ion detection (or $[M-H]^-$ for negative ion detection) were calculated for all the phospholipids detected by FTICR MS in the phospholipid molecular profiling experiments. These m/z values were used to locate the individual phospholipid species in the LC/MS profiles and to determine their retention times (RTs) in each ion mode. Using these m/z-RT pairs, a QuanLynx quantitation method was generated for each ion mode with customized peak detection, integration and smoothing parameters for each peak, taking into account peak symmetry and tailing, to extract the ion current chromatograms of all the mass-matched phospholipids. Peaks were only integrated if the peak area was ≥ 3 and detectable in at least 9 of the total 18 samples (50% of samples) or in at least 8 of the total 18 if the detectable peak areas were present in all 8 control group samples. For all extracted ion current chromatograms, a mass window of 50 ppm and a retention time shift of 0.10 min were used to assign a unique species during data extraction. QuanLynx integrated the peak closest to the retention time entered. The extracted ion chromatograms were smoothed using the moving mean approach with a smoothing width of 3 and a smoothing iteration of 2. Peak integrations were checked for each species to ensure that peak extraction was performed correctly, with some necessary manual intervention. The extracted peak areas were then exported into Microsoft Excel and the corresponding neutral mass-retention time pairs were recorded for each set of peak areas. In this way, a separate Microsoft Excel file was generated for each ionization mode. The spreadsheets were then saved in a text file format amenable to multivariate and univariate statistics.

These unique, quantitated phospholipid masses detected by QTOF MS (220 masses for both ion modes combined) were separated into 9 phospholipid classes. These classes were: CerP, PA, PC, PC/PE, PE, PG, PI (including PIP), PS and SM. This phospholipid class distribution is shown in Table 1. To determine a possible bias in the results due to the method used, the phospholipid class distribution of these 220 quantitated phospholipid masses detected by QTOF MS was compared to that of the 488 phospholipid masses detected by FTICR MS. This was done by dividing the number of unique, QTOF MS-detected phospholipid masses in each class by the number of FTICR MS-detected unique phospholipid masses in each class. This fraction was then expressed as a percentage. This was termed the "quantitation percentage" and is shown in the last column of Table 1.

3.2.5. Multivariate Statistics

SimcaP+ 11.5 (Umetrics AB, Umeå, Sweden) was used for data modeling using multivariate analysis approaches, including unsupervised principal component analysis (PCA) and supervised partial least squares-discriminant analysis (PLS-DA). The coefficient of determination (R^2), cross-validated R^2 (Q^2), and Variable Importance Plot (VIP) were used to evaluate the contributions of each principal component (PC), to the fitted models derived from PLS-DA. The R^2 value is the fraction of variance (sum of squares) explained by the model. The Q^2 value is the fraction of the total variation of each sample groups that can be predicted by a component. VIP quantified the normalized contribution of each of the variables (*e.g.*, mass-retention time pairs) to sample separation. The VIPs of the PLS-DA model were examined for largest variable importance score. In this way, the phospholipid species corresponding to the top 10 scores in each ionization mode were selected for further structural confirmation by MS/MS experiments. These selected phospholipids were termed the "top 20 phospholipid masses". These top 20 phospholipid masses were categorized into their respective phospholipid classes (as described for the 220 quantitated phospholipids in the "Data Processing" section) and are shown in Table 1. Peak areas for all top 20 phospholipid masses were then subjected to univariate statistical analysis.

3.2.6. Univariate Statistics

In order to determine whether the differences in phospholipid abundance were statistically significant, univariate statistics were conducted, either in Microsoft Excel or by using Minitab 16 (Minitab Inc., State College, PA, USA). Box-plots were generated for the top 20 phospholipids to better visualize data distribution and to detect possible outliers. If any outliers were detected, they were excluded from the calculations for all subsequent statistical analysis. In order to ensure that the parameter assumptions of the t-test were met, samples groups were tested for normality and sample group variances were tested for similarity. To test for normality, a Ryan-Joiner test (similar to a Shapiro-Wilk test) was used and the corresponding P-value reported. To test for similarity of sample variances for the top 20 phospholipids at the 95% confidence level, Levene's test was performed. The P-value associated with Levene's test was also reported. The two sample-group means for each of the top 20 phospholipids were then

checked for statistical significance using the two-tailed t-test approach. Based on the results of the Levene's tests, if sample variance was found to be equal, a two tailed t-test for similar variances was performed. If sample variance could not be deemed to be equal, a two tailed t-test for unequal variances was performed. The results of these univariate statistical tests are listed in Appendix B.

3.2.7. Structural Characterization by MS/MS and Accurate Mass

Offline UPLC fractionation and DI/MS/MS using collision cell CID on the FTMS instrument were performed to confirm the structural identities of the top 20 statistically significant phospholipids as determined by PLS-DA. To do this, LLE was performed on a healthy human plasma sample (from a 47-year-old female) obtained from Innovative Research using the same sample preparation protocol and LC conditions described above in the "Sample Preparation" section of this chapter. The UPLC conditions were the same as those used for the UPLC/QTOF MS metabolic analysis. However, after UPLC separation, 30-s fractions were collected at the outlet of the UPLC column using a Foxy 200 automatic fraction collector (Teledyne ISCO, Lincoln, NE, USA). The fractions of interest were located based on RTs obtained during the LC/MS runs described in the "3.2.3. UPLC/QTOF MS" section above. The fractions of interest were then re-infused into the FTICR MS instrument with aid of a KD Scientific syringe pump at a flow rate of 2 μL/min. The precursor ions for the phospholipids of interest were selected by quadrupole 2 (as a mass filter) as shown in Figure 6, typically with a mass window of +/- 0.5 Da around the central m/z values. Precursor ions were accumulated in the hexapole collision cell until a survey scan signal intensity of > 4~5 x 10^6 was reached in order to accumulate a sufficient number of ions for fragmentation; MS/MS was induced by CID in the collision cell by applying bias voltages as collision energy and with argon as the collision gas. The resultant product ions were finally guided into the ICR cell by the ion transfer optics, where they were subjected to ion trapping, excitation, and detection. Five phospholipids in total could be assigned a single unique phospholipid structure. This included one phospholipid identified by this MS/MS approach. The remaining 4 phospholipid masses each matched a single phospholipid structure each in the LIPID MAPS database.

3.3.Results

3.3.1. Data Extraction

After targeted mass-directed data processing using QuanLynx, in addition to some necessary manual intervention, 134 phospholipid-specific m/z-RT pairs were generated and extracted from the UPLC/MS dataset acquired in the positive ion mode. For the UPLC/MS dataset acquired in the negative ion mode, 157 phospholipid-RT pairs were extracted. This corresponded to 102 and 128 unique phospholipid masses in positive and negative ion modes, respectively, if multiple RTs for the same phospholipid mass were excluded (to maintain consistency for comparison with the FTICR MS-detected matched phospholipid masses described later). Figure 10 shows 4 representative LC/MS chromatograms acquired from one MetS patient sample and one control sample in both positive and negative ion modes. Figure 11 is an excerpt of each of the generated two-dimensional data matrices showing the peak area values for phospholipid-specific m/z-RT pairs obtained after batch data extraction of the LC/MS chromatograms.

Table 1 displays the distribution of phospholipid classes assigned at different data processing/analysis stages: 488 unique masses matching at least one phospholipid mass in LIPID MAPS; 220 m/z-RT pairs extracted from UPLC/QTOF MS datasets, and the top 20 most significant species concluded from PLS-DA data modeling. Using the FTICR MS-derived 488 unique masses, 220 of these were successfully quantitated from the two UPLC/QTOF MS datasets acquired in positive and negative ion modes. This equates to an overall phospholipid quantitation percentage of approximately 45%. Further analysis of the quantitated mass-RT pairs within each of the 9 phospholipid classes revealed a quantitation percentage for each of these phospholipid classes. The approximate quantitation percentage of 51% for the class PS was similar to the overall quantitation percentage of 45%. The percentage of total phospholipids quantitated was high for 4 of the phospholipid classes: PC (67%), PC/PE (81%), PE (69%), and SM (80%). Conversely, the percentage of phospholipids quantitated was somewhat low for 4 of the phospholipid classes: CerP (0%), PA (21%), PG (27%) and PI (9%). As shown in figure 8, an intra-group comparison of the total 488 masses detected by FTMS reveals the following phospholipid quantitation percentage by class, in order of descending percentage as follows: PS

(18.9%), PC/PE (17.0%), PA (15.0%), PG (13.1%), PI (13.1%), PC (9.8%), PE (7.2%), SM (3.1%), and CerP (2.9%).

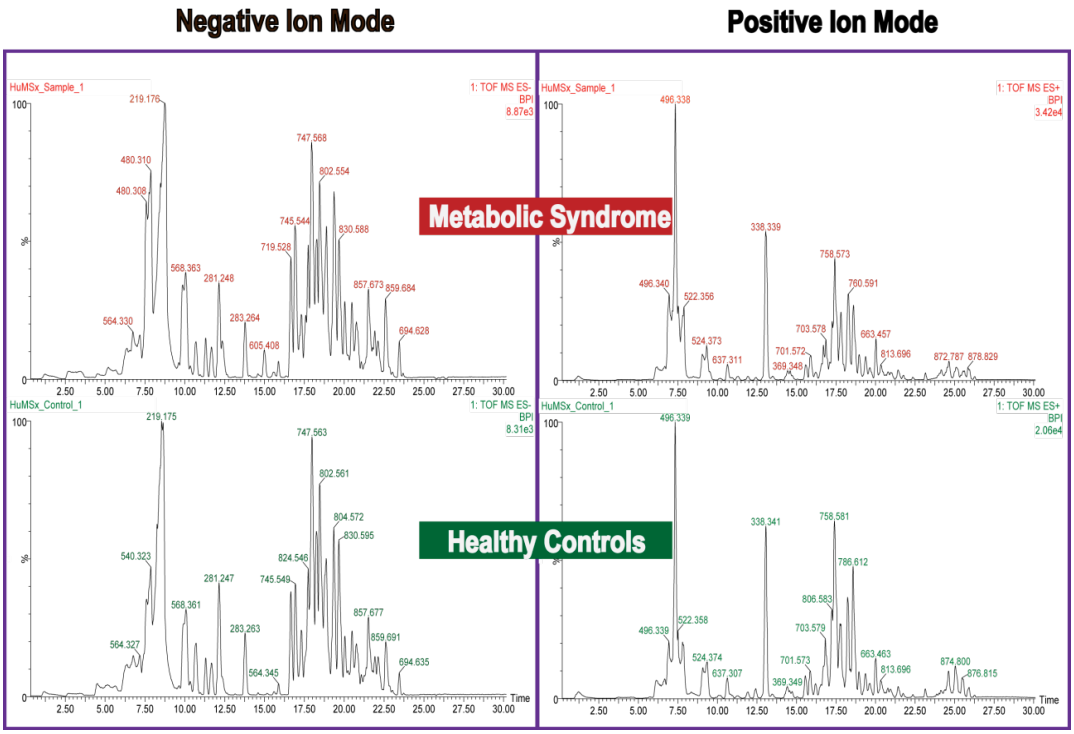

Figure 10. Representative LC/MS Chromatograms Acquired by QTOF MS.
Two representative chromatograms (MetS in the upper panels, lean healthy controls in the lower panels) are shown for each ionization mode. While some differences in chromatographic peaks are readily apparent, the chromatograms in each ion mode appear very similar. The data from these chromatograms must be extracted with the use of software in order to maximize the information obtained from these chromatograms.

	453.2855_7.5	467.3012_4.8	467.3012_5.5	479.3376_7.8	481.3168_6.4	481.3168_9.6	481.3532_7.7
MetS1	11.947	32.282	21.335	90.107	15.754	20.376	76.055
MetS2	8.014	11.962	16.266	54.597	10.216	15.476	53.196
MetS3	5.694	28.059	32.892	73.409	22.258	14.479	85.766
MetS4	8.334	40.636	29.172	113.082	17.949	18.147	97.983
MetS5	8.696	23.634	12.15	54.6	15.706	17.832	47.089
MetS6	11.144	34.624	30.625	98.091	15.704	17.391	82.335
MetS7	6.195	18.814	18.74	68.837	14.156	12.56	70.703
MetS8	6.932	14.303	20.666	90.381	15.57	17.304	109.142
MetS9	10.251	32.623	32.394	89.591	8.712	18.983	79.149
MetS10	4.022	14.487	15.278	45.379	10.092	9.376	45.997
Control1	7.53	8.471	15.345	65.875	11.685	15.787	108.697
Control2	6.98	18.513	17.577	67.333	11.929	12.438	57.379
Control3	6.749	17.137	19.43	65.656	14.145	15.131	57.525
Control4	9.936	15.908	15.669	59.827	16.841	13.615	67.149
Control5	8.638	13.926	11.288	57.671	9.413	15.256	81.983
Control6	9.037	14.683	20.091	66.576	15.256	14.143	79.401
Control7	5.699	12.782	14.814	55.88	11.128	12.349	43.288
Control8	6.423	11.976	11.7	56.978	9.561	13.167	61.398

	396.2277_10.4	453.2855_5.4	453.2855_8.1	465.3219_8.4	465.3219_11.4	467.3012_6.5	477.2855_7.4
MetS1	6.469	51.574	76.584	18.878	14.479	24.154	56.194
MetS2	11.718	32.609	54.997	13.234	13.831	23.838	35.895
MetS3	4.64	63.734	40.575	13.665	13.748	43.798	57.012
MetS4	5.786	83.497	62.531	23.825	11.797	41.664	56.631
MetS5	4.216	28.738	47.733	10.025	11.1	22.287	40.029
MetS6	11.486	62.994	63.503	20.546	11.531	21.186	29.553
MetS7	6.481	40.251	40.965	11.066	7.261	29.635	53.508
MetS8	4.413	36.957	42.865	14.184	15.393	24.185	36.169
MetS9	13.284	51.137	54.807	16.55	9.313	11.122	39.314
MetS10	3.628	32.895	32.068	10.835	5.962	15.954	50.648
Control1	12.163	25.326	48.667	10.294	23.646	22.655	34.604
Control2	5.119	39.705	51.304	16.309	8.76	25.153	44.547
Control3	4.963	41.168	45.668	11.404	11.591	22.82	53.458
Control4	6.521	37.668	62.777	11.216	10.141	19.683	73.485
Control5	7.279	25.09	49.416	7.661	13.381	16.807	22.765
Control6	12.26	41.43	59.424	15.583	12.748	33.133	35.043
Control7	3.635	31.096	39.339	10.873	9.753	18.94	52.917
Control8	9.069	23.846	39.517	9.565	7.762	21.059	32.113

Figure 11. Representative Data Extracted from LC/QTOF MS Chromatograms. An excerpt of peak areas extracted from LC/MS chromatograms acquired in positive ion mode (upper panel) and negative ion mode (lower panel). Each column of peak areas is labelled with its respective neutral mass and retention time pair (separated by an underscore).

3.3.2. Multivariate Analysis

For the data acquired in the positive ion mode, automated model fitting using PLS-DA calculated a cumulative R^2 value of 0.937 and a cumulative Q^2 value of 0.466 for the first 3 principal components, as shown in Figure 12. For the data acquired in the negative ion mode, a cumulative R^2 value of 0.970 and a cumulative Q^2 value of 0.724 were calculated for the first 3 principal components. Figure 13 shows two scores plots of PLS-DA for the extracted data matrices from the positive and negative ion LC/MS datasets. As shown, the PLS-DA score plots revealed clear separations between the MetS group and the healthy control group for both the positive and negative ion datasets. All of the MetS and control samples lie within the boundaries of the plotted Hotelling T^2 ellipse at a 95% confidence level. The VIP plots for the top 10 most

significant contributors to the group separation for each ionization mode are shown in Figure 14. The VIP values are roughly similar for data acquired in the positive ion mode *vs.* negative ion mode. Both of these VIP plots show that for each of these top 20 phospholipids, the VIP value is greater than 1.5. In addition, there is no overlap between the top 10 contributing phospholipids in the positive ion mode *vs.* the top 10 in the negative ion mode. Figure 15 displays the average peak areas and the corresponding standard errors of the means (error bars) for the top 10 phospholipids that contributed the most to the PLS-DA group separation detected in the positive ion mode. Figure 16 shows the average peak areas and the corresponding standard errors of the means (error bars) for the top 10 phospholipids contributing most to PLS-DA group separation detected in negative ion mode. Six phospholipids in each ionization mode were detected at higher relative abundance in the LC/MS profiles, and are therefore plotted in two separate graphs solely for the sake of improved visualization.

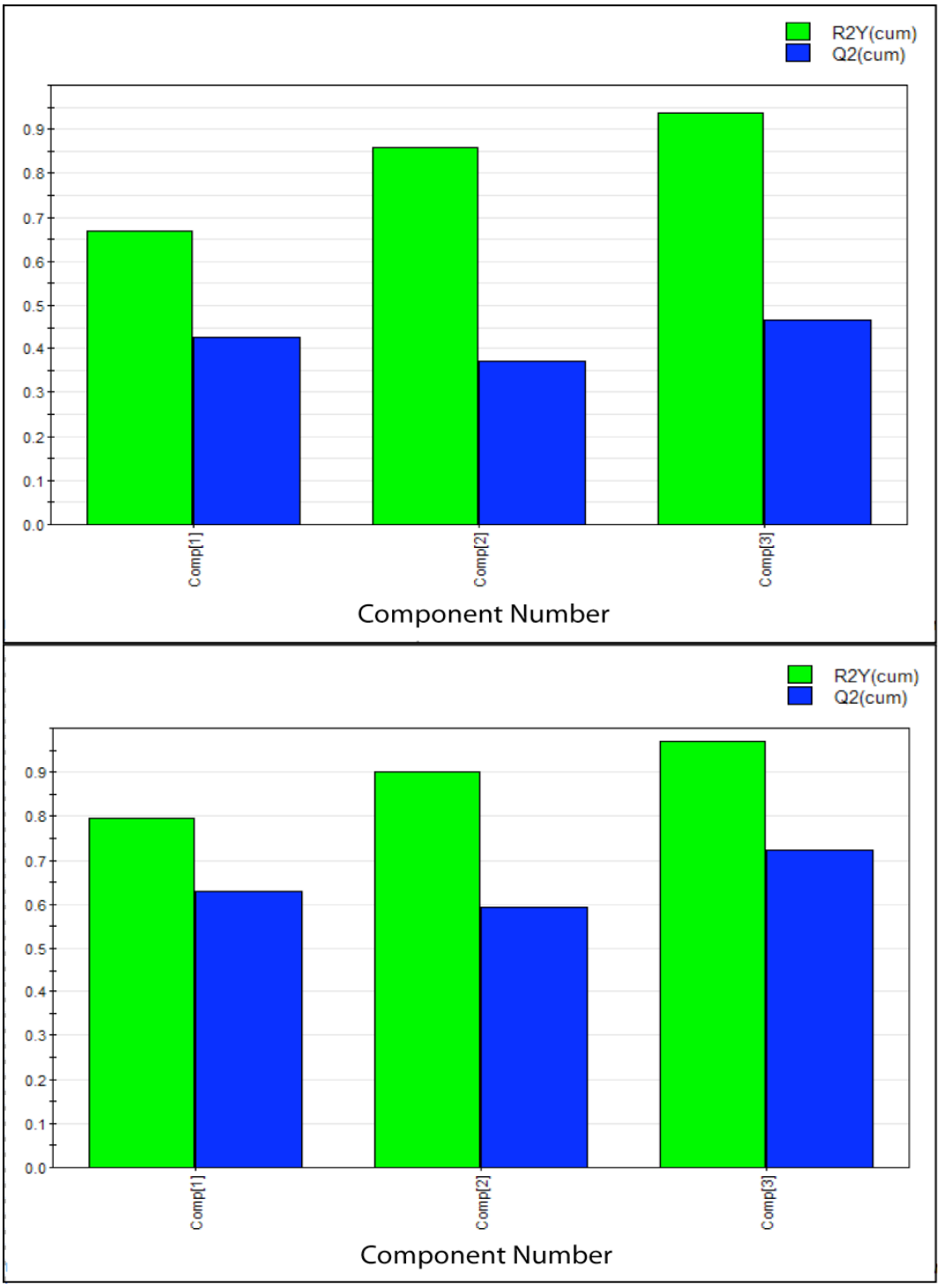

Figure 12. Fit of Statistical Models Used for Multivariate Analysis (PLS-DA). Values for model parameters R^2 and Q^2 after 3 components in both positive ion mode (upper panel) and negative ion mode (lower panel) show good PLS-DA-model fit.

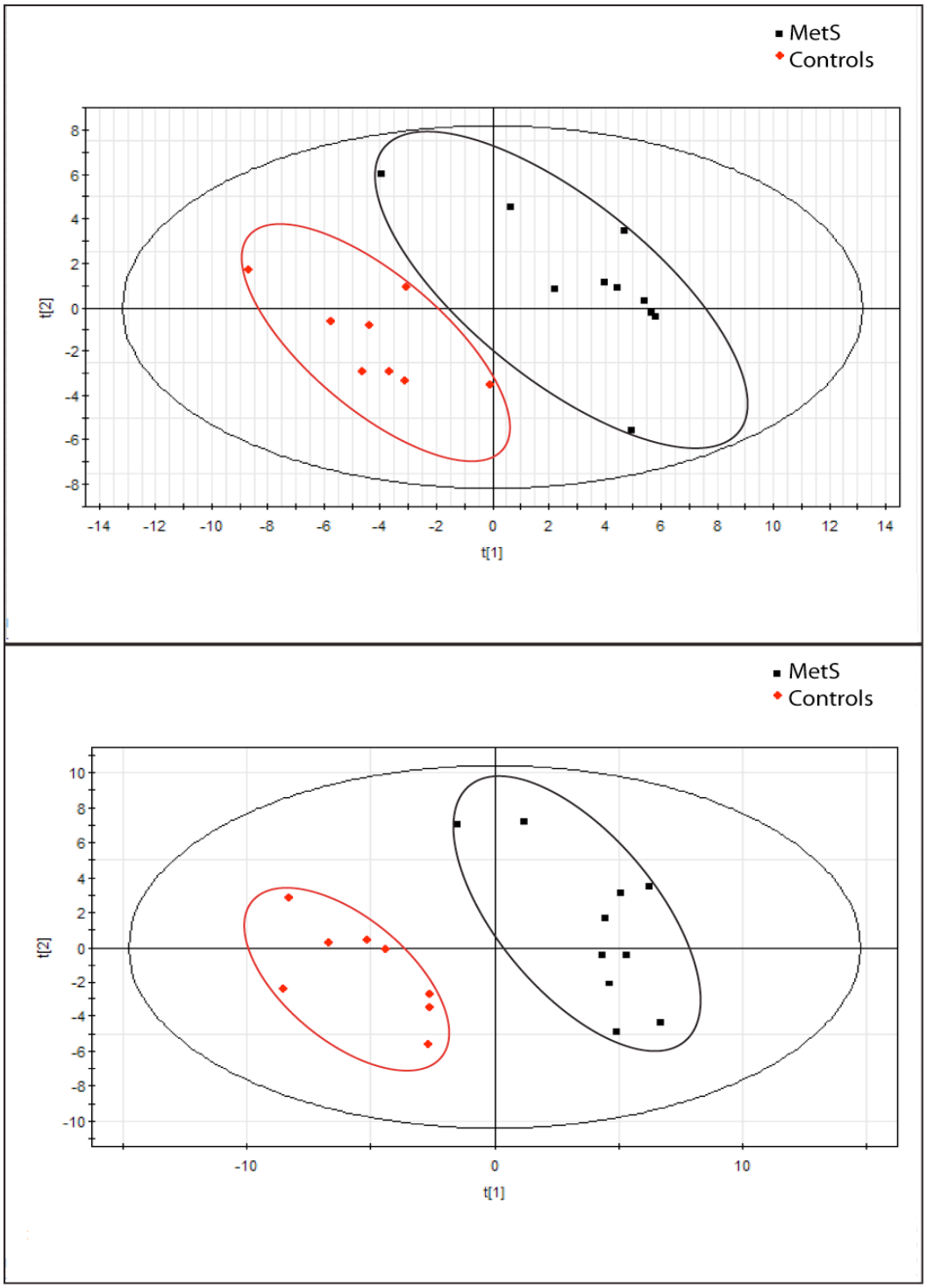

Figure 13. PLS-DA Scores Plots for MetS *vs.* Healthy Controls.
PLS-DA scores plots for data acquired in both positive (upper panel) and negative (lower panel) ion modes both show clear separation between the MetS group and the healthy control group. PLS-DA was able to distinguish a difference in the phospholipid abundances of plasma samples from individuals with MetS from those of lean, healthy controls at the 95% confidence level.

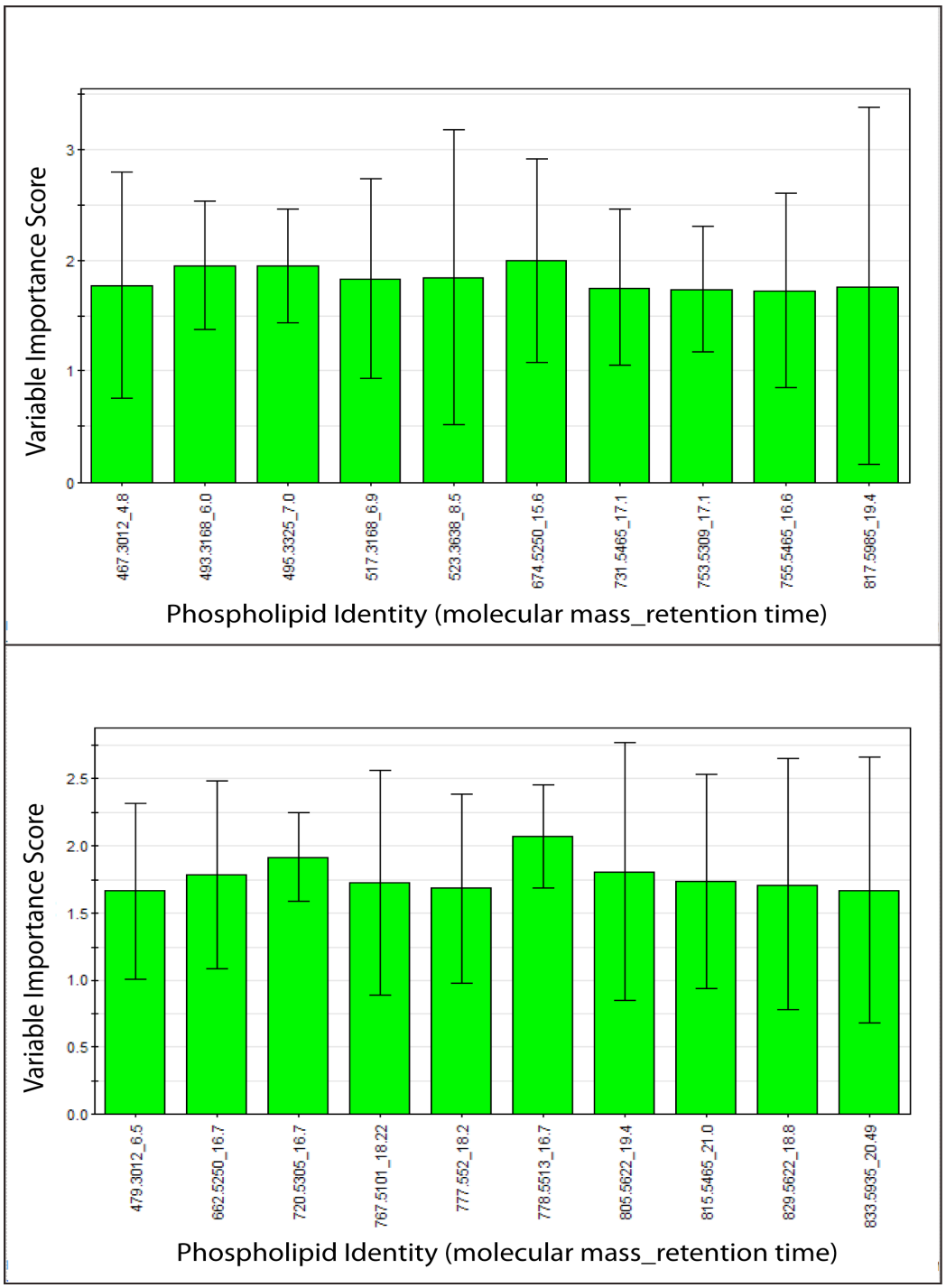

Figure 14. Variable Importance Plots for Top 10 Phospholipids From PLS-DA.
Bar graph showing the variable importance scores for the top 10 phospholipid mass-retention time pairs in positive ion mode (upper panel) and negative ion mode (lower panel) which contributed the most to the separation between the MetS group and the healthy control group detected by PLS-DA. The error bars represent confidence intervals at the 95% confidence level.

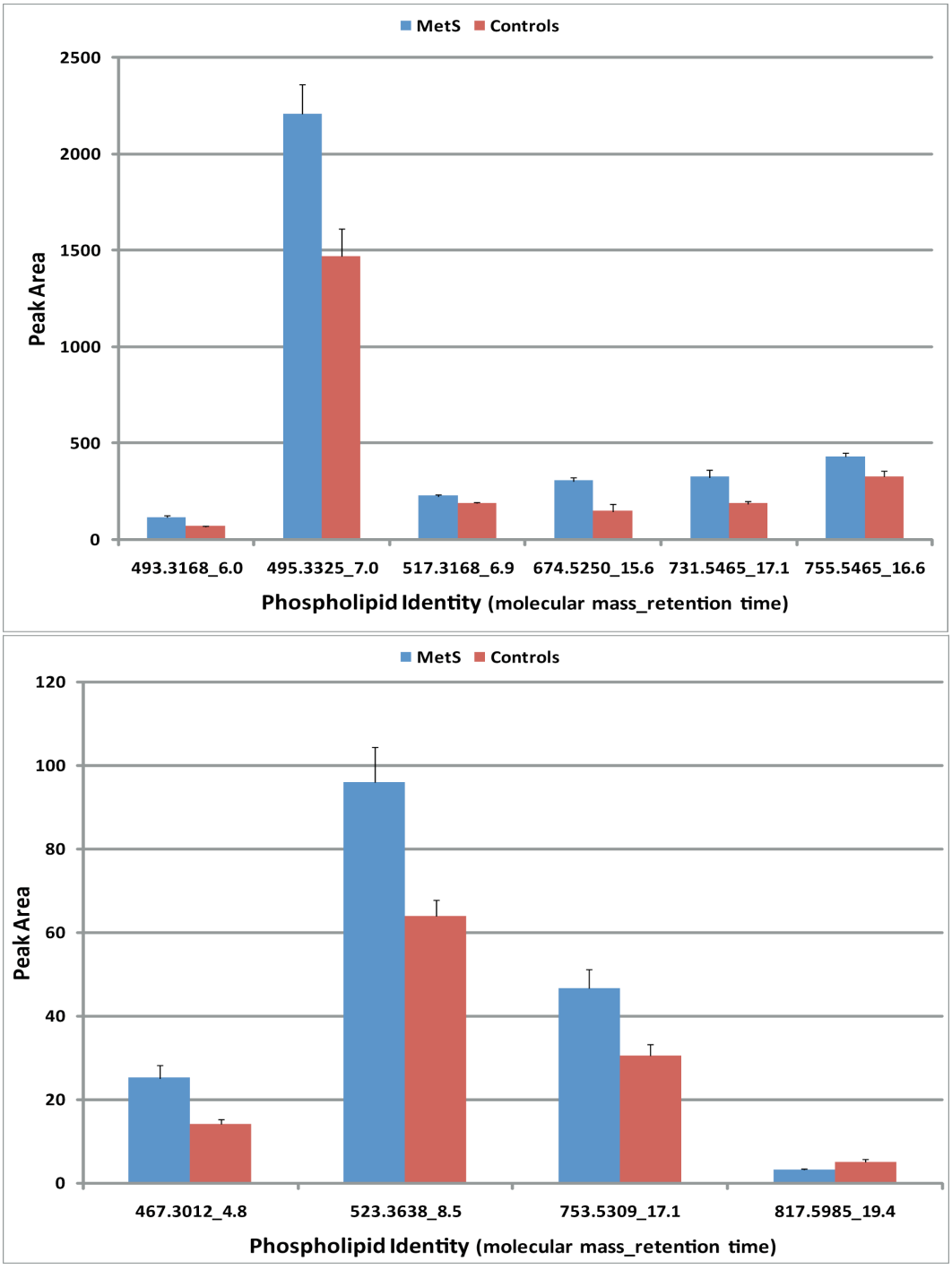

Figure 15. Abundances of Top 10 Phospholipids Detected in Positive Ion Mode by LC/QTOF MS.

Bar graphs displaying peak area averages for MetS and healthy control groups for data acquired in positive ion mode. For each peak area average, the standard error of the mean is also plotted. One of the top 10 most significant phospholipids in positive ion mode was found in lower abundance in MetS samples than in samples from healthy controls.

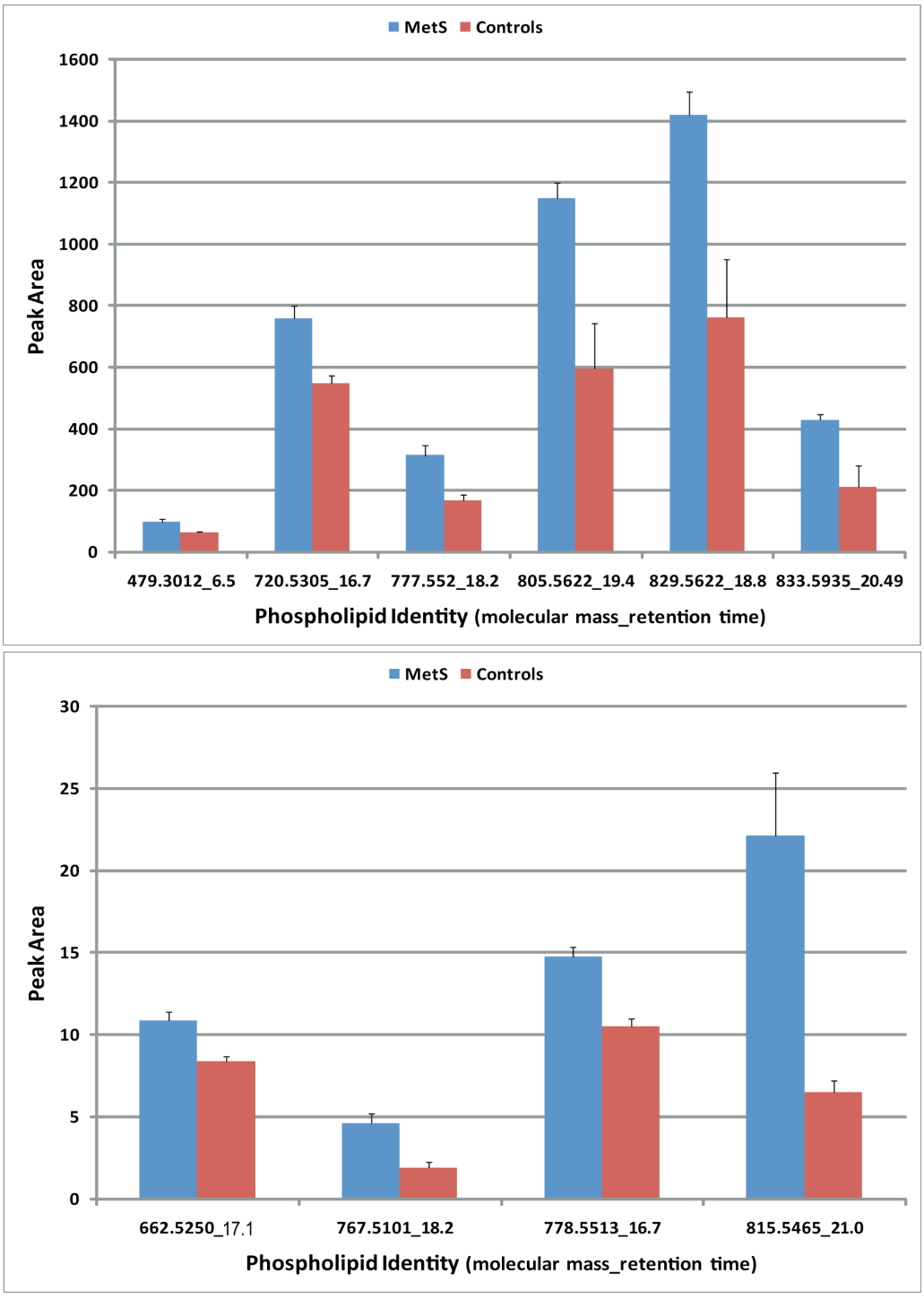

Figure 16. Abundances of Top 10 Phospholipids Detected in Negative Ion Mode by LC/QTOF MS.

Bar graphs displaying peak area averages for MetS and healthy control groups for data acquired in negative ion mode. For each peak area average, the standard error of the mean is also plotted. All top 10 most significant phospholipids in negative ion mode were found in higher abundance in MetS samples than in samples from healthy controls.

3.3.3. Univariate Analysis

Figure 17 and 18 display the box-plots for the peak areas of the top 20 phospholipids. The phospholipid corresponding to 495.3325 Da is shown as an inset graph solely due to differences in peak area scaling. This was done to aid visualization of the box plots for lower abundance phospholipids. One outlier was detected by Minitab in the data acquired in negative ion mode, as displayed in Figure 18, shown as an asterisk lying outside the box plot maxima. An outlier, as defined by Minitab, represents an observation that is at least 1.5 times the value of the interquartile range away from the interquartile range minimum or maximum (either the top edge or bottom edge of the box in a box plot). The outlier detected corresponded to the phospholipid 777.5520_18.2 (outlier from control sample 13). After verifying correct peak area integration, this outlier was removed from calculation in univariate statistical tests. The results of the Ryan-Joiner tests, Levene's tests and t-tests can be found in Appendix B. Ryan-Joiner tests for all phospholipids returned P values > 0.100 at the 95% confidence level. The P values from the Levene's test used to determine similar variances are also shown in Appendix B. As shown, the Levene's tests returned P values < 0.05 for 8 phospholipids at the 95% confidence level. The remaining 12 of these 20 phospholipids returned P values > 0.050 for the Levene's tests at the 95% confidence level. Also shown in appendix B are P values for independent, two sample, two-tailed t-tests at the 95% confidence level. These t-test P values are all ≤ 0.016. In fact, 17 of the 20 phospholipids had associated P values ≤ 0.010 for the t-test. The detected difference in abundance between MetS and healthy controls was found to be statistically significant for all of the top 20 phospholipids.

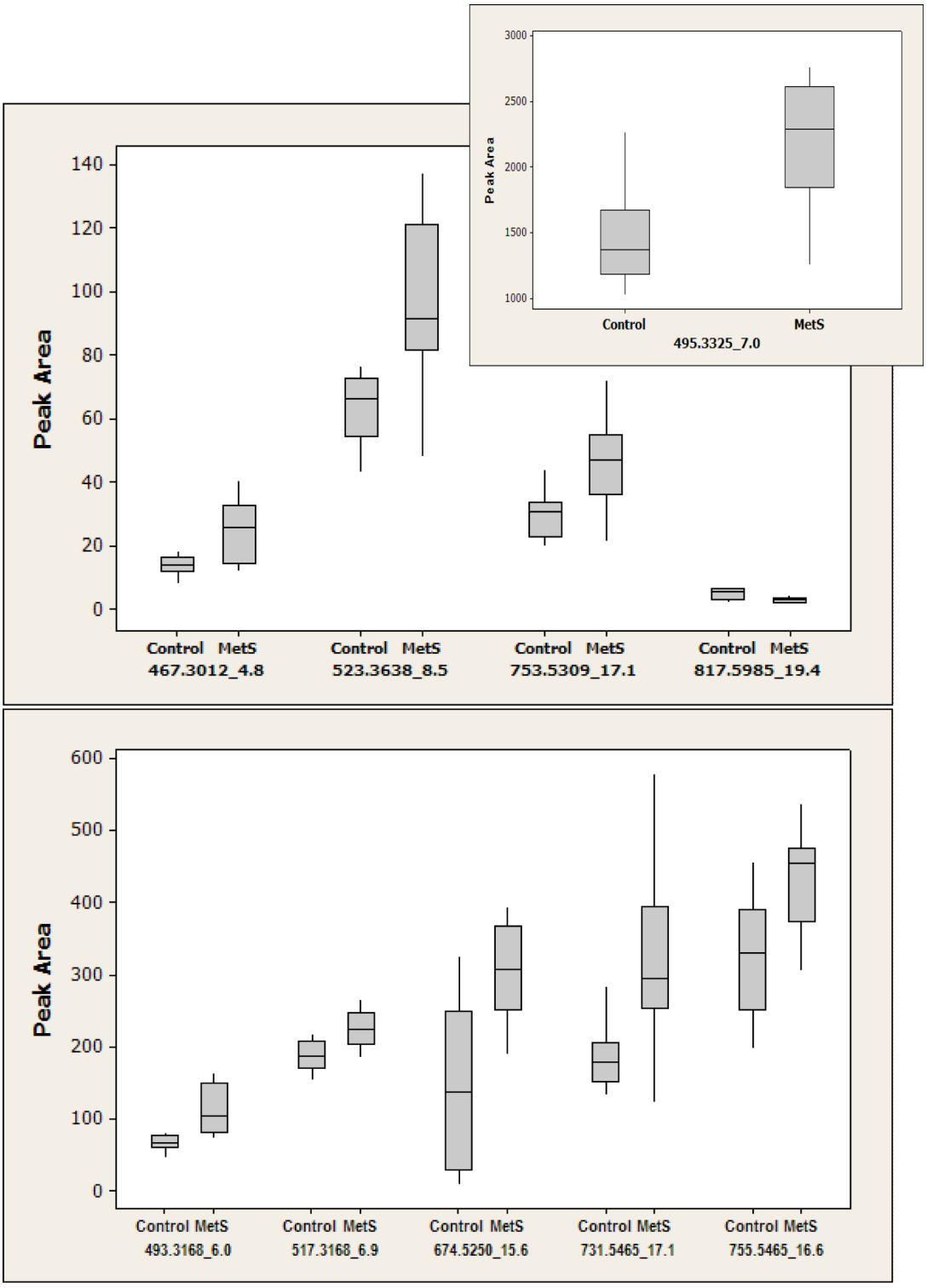

Figure 17. Distribution of QTOF MS Extracted Data for the Top 10 Phospholipids in Positive Ion Mode.

Box plots illustrating the distribution of peak areas for all 10 phospholipids contributing most to PLS-DA group separation in positive ion mode are shown. A distinct difference in the interquartile ranges of peak area values between groups is visible for 2 of these 10 phospholipids.

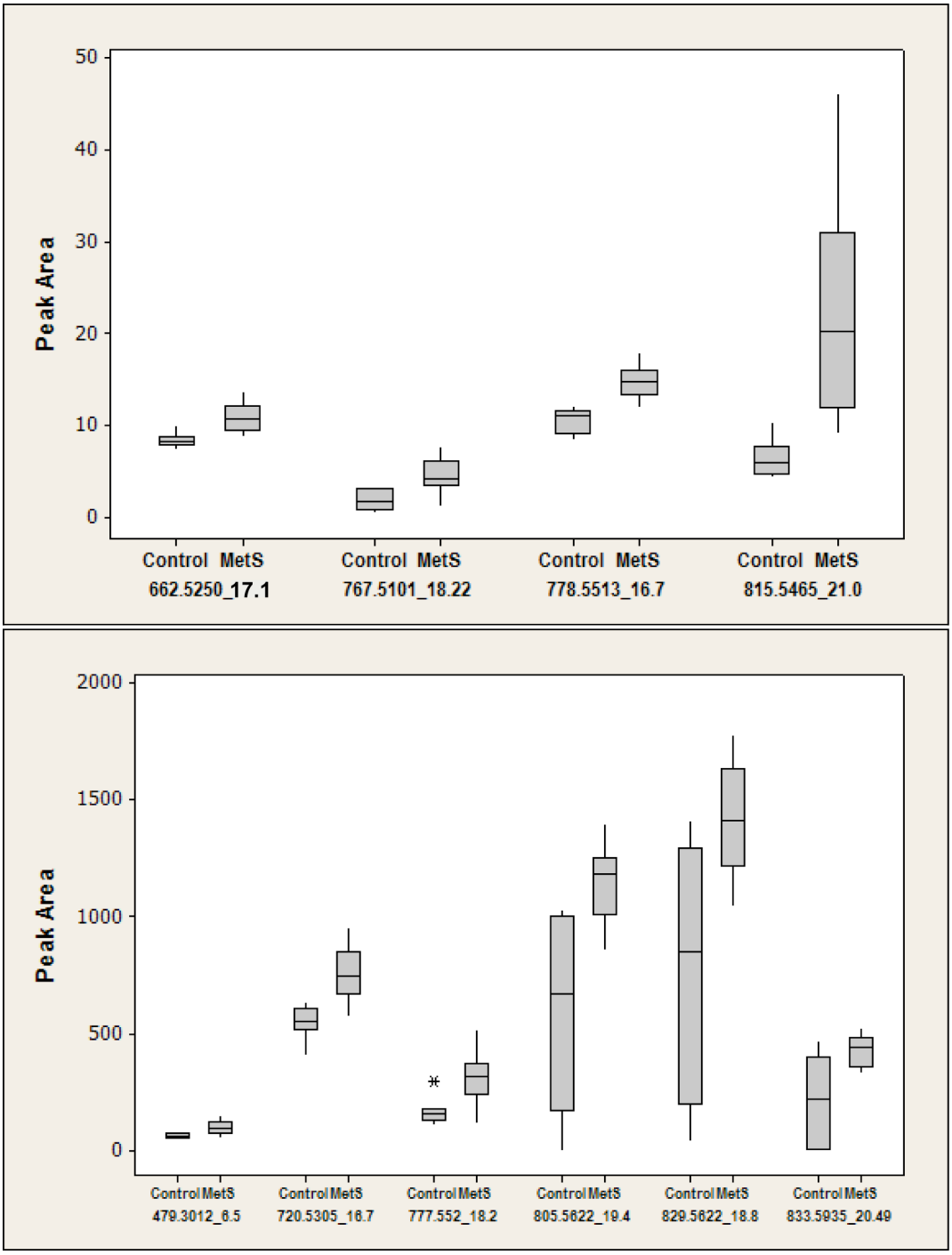

Figure 18. Distribution of QTOF MS Extracted Data for the Top 10 Phospholipids in Negative Ion Mode.

Box plots illustrating the distribution of peak areas for all 10 phospholipids contributing most to PLS-DA group separation in negative ion mode are shown. A distinct difference in the interquartile ranges of peak area values between groups is visible for 7 of these 10 phospholipids. The outlier is displayed as an asterisk.

3.3.4. Structural Characterization by MS/MS and Accurate Mass

Offline UPLC fractionation and DI/FTMS/MS were used for structural identification for the top 20 species revealed by PLS-DA data modeling. Among these 20 species, 16 matched more than one phospholipid species in the LIPID MAPS database. This included the phospholipid corresponding to neutral mass of 495.3325 Da. A search of LIPID MAPS using 495.3325 Da within a mass error of 6 ppm returned two phospholipid species. One of these phospholipid species was PE (19:0/0:0) and the other was PC (16:0/0:0). The phospholipid representing this neutral mass of 495.3325 Da was detected in (+) ESI mode on the UPLC/QTOF MS profiles at 7.0 min, corresponding to an $[M+H]^+$ ion at 496.3398 Th. To structurally identify this phospholipid, an MS/MS spectrum corresponding to 496.3398 Th was successfully acquired by CID following ion isolation with quadrupole mass filter using an isolation mass window of 1 Th around 496.3398 Th. Figure 19 shows the MS/MS spectrum corresponding to this phospholipid species. The fragment ion at m/z 258.1099 Th and its dehydrated counterpart at m/z 240.0994 Th indicated the existence of an acyl chain corresponding to 16:0, but not 19:0. In addition, an ion at m/z 184.073 Th was also observed, indicating the existence of at least one phosphocholine group in this molecule. Therefore, the phospholipid mass of 495.3325 Da was assigned to PC (16:0/0:0), not PE (19:0/0:0). For the remaining 19 species, however, no good MS/MS spectra were acquired due to their very low abundances observed on the survey scan mass spectra. Of these 19 species, 4 matched only one unique phospholipid *structure* each from a search of the LIPID MAPS database using their accurate masses. These 4 mass-matched phospholipid masses are 479.3012 Da (PE(18:1/0:0)), 493.3168 Da (PC(16:1/0:0)), 517.3168 Da (PC(18:3/0:0)), and 817.5985 Da (PC(18:0/22:6)). These 4 phospholipids are listed in Table 3 along with the phospholipid that was structurally characterized by MS/MS.

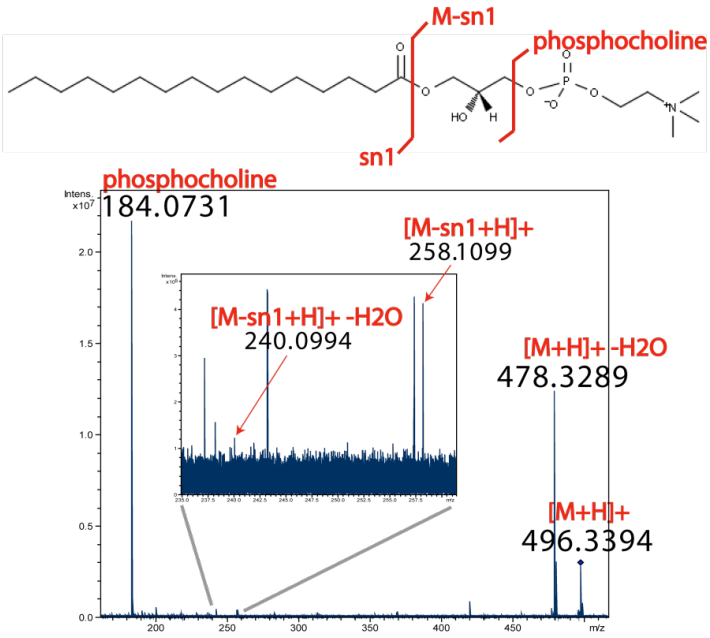

Input Mass	Matched Mass	Delta	HG	C	DB	Abbreviation	M-sn1	M-sn1-H2O	M-sn2	M-sn2-H2O	Formula	Ion
496.3394	496.3398	.0004	PC	16	0	PC(16:0/0:0)	258.1101	240.0995	-	-	$C_{24}H_{51}NO_7P$	[M+H]+
496.3394	496.3398	.0004	PE	19	0	PE(19:0/0:0)	216.0632	198.0526	-	-	$C_{24}H_{51}NO_7P$	[M+H]+

Figure 19. Confirmation of Phospholipid Structure Using FTICR MS/MS.
LIPID MAPS matched neutral mass 495.3325 Da to two possible phospholipid species in the database. After detection in positive ion mode, MS/MS revealed the structural identity of the phospholipid corresponding to molecular mass 495.3325 Da to be PC (16:0/0:0).

Table 3. Structural Identities of Molecularly Characterized, Statistically Significant Phospholipids. The structural identities for all 5 phospholipid masses with statistically-significant differences in abundance between MetS and healthy controls and that could be assigned a single phospholipid structure are shown below. One of these phospholipids was found at lower abundances in MetS *vs.* healthy controls; 4 of these were found at higher abundances in MetS patients.

Molecular Wt. (Da)	Abbreviated Phospholipid ID	Change in MetS	Chemical Formula	Molecular Structure
479.3012	PE(18:1/0:0)	↑	$C_{23}H_{46}NO_7P$	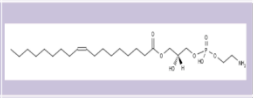
493.3168	PC(16:1/0:0)	↑	$C_{24}H_{48}NO_7P$	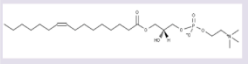
495.3325	PC(16:0/0:0)	↑	$C_{24}H_{50}NO_7P$	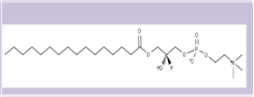
517.3168	PC(18:3/0:0)	↑	$C_{26}H_{48}NO_7P$	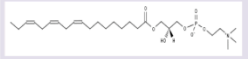
817.5985	PC(P-18:0/22:6)	↓	$C_{48}H_{84}NO_7P$	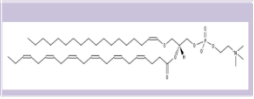

3.4. Discussion

3.4.1. Sample Preparation

In this experiment, the sample preparation protocol for LC/MS relative quantitation was almost identical to that used for the FTMS molecular profiling experiments, so that the results would be comparable. The only difference was the composition of the solvent in which samples were diluted immediately prior to analysis. The lower percentage organic as compared to that used in profiling experiments was found to aid in the peak shape and resolution of early-eluting compounds. The solvent composition used for LC injection was the lowest percent of organic (IPA) in which the extracted lipids would dissolve.

3.4.2. Sample Analysis

The LC/MS technique used in this study combined the advantages of UPLC and high-resolution QTOF MS. One of the benefits of UPLC for sample analysis is the excellent retention time reproducibility. With UPLC/QTOF MS, most of the phospholipids detected showed RT

shifts of < 0.1 min. This good RT reproducibility offered an added level of confidence for location, integration, and alignment of the correct peaks across all samples during data processing. In addition, the use of a lock mass spray helped to improve the mass accuracy of the QTOF mass spectrometer by providing a reference mass for dynamic internal mass calibration. In this way, a mass window of 50 ppm (*i.e.*, +/- 25 ppm) around the central m/z values, was shown to be sufficient to extract all the phospholipids throughout the entire set of LC/MS profiles.

IPA/ACN (2:1, v/v) was used for the organic mobile phase in these experiments. Compared to ACN alone, the addition of IPA to the mobile phase improved the solvent strength for elution of all phospholipids from the UPLC column, especially for less-polar and neutral lipids, thus greatly reducing the sample carry-over. This made quantitative sample-to-sample comparisons more accurate, reproducible, and reliable.

3.4.3. Data Processing

During method development, untargeted data extraction using MarkerLynx, a software program within the Waters MassLynx suite, was used for tentative peak detection, integration, and alignment. The automatically-extracted metabolite features were then checked manually. However, it was found that, after many iterations of parameter optimization for proper data extraction (by trial-and-error) using MarkerLynx, the data was still being extracted incorrectly for most peaks. In part, this was most likely due to the extreme complexity of the LC/MS metabolomic data files.

MarkerLynx only allowed a user to use a single set of parameters for peak detection, integration and alignment; the algorithms underlying these processing methods are not transparent to users. Thus, the effect a parameter has on data extraction is unclear. This means that a trial-and-error approach to parameter optimization is sometimes necessary, and researchers are forced to adjust parameters based on the expected outcome. However, this approach to parameter optimization could clearly add scientific bias to the data analysis. This suggests a need for more intuitive software and/or more clearly-established standardized guidelines for unbiased data extraction and analysis. Also, as previously mentioned, the metabolomic datasets derived from untargeted analysis of complex biological samples by LC/MS, are extremely

complex and this adds to the difficulty of the data extraction process used for untargeted metabolomics.

Considering these factors, a targeted, mass-directed, data extraction approach was used instead. The theoretical monoisotopic m/z values of the potential human plasma phospholipids, as determined by FTICR MS were used to locate the positions of these possible phospholipids in the UPLC/MS profiles. The m/z-RT pairs were then used to compile QuanLynx methods for targeted extraction of the detectable phospholipids from the UPLC/QTOF MS datasets. Although this approach is slightly more time-consuming, the results were shown to be more reliable when compared to untargeted data extraction using MarkerLynx alone. This is because, in QuanLynx, the set of parameters used for detection, integration, and alignment of any peak can be individually customized, depending on the observed peak shape characteristics, including peak broadening, tailing, shouldering, and even partial chromatographic resolution. In addition, manual correction of incorrectly extracted data can be methodically and thoroughly conducted when using QuanLynx. This targeted, mass-directed data extraction ensured reliable data processing in these experiments and prepared the data for subsequent analysis using multivariate and univariate statistics in order to determine quantitative differences between MetS and healthy controls attributable only to phospholipids (rather than neutral lipids, other metabolites, peptides etc.).

As shown in Table 1, approximately 45% of phospholipid masses detected by FTICR MS were quantitated. The quantitation percentage of 51% for the phospholipid class PS suggests there was minimal class selection bias from the analytical method used for these QTOF MS experiments as it is fairly close to the average value of 45% for phospholipids quantitated. However, the fact that the quantitation percentages of 67%, 81%, 69% and 80% for PC, PC/PE, PE and SM respectively are significantly higher could mean that individual phospholipids were present in higher concentrations in plasma relative to the plasma concentrations of phospholipids belonging to the remaining classes. Alternatively, these increased values could be suggestive of increased ionization efficiency relative to other phospholipids, thus effectively increasing the detection of PC and SM. Either of these effects individually or in combination would increase the likelihood that these phospholipids would meet the cut-off criteria for peak integration, thereby elevating the quantitation percentage. This can be accounted for by the reason that both PC and SM contain a choline head group which would generate strong ESI-MS signals in

positive ion detection mode. Due to the low abundance and/or ionization efficiency of many of the phospholipids in the human plasma samples, only 220 peaks from the 488 unique phospholipid masses were detected with sufficient peak areas for quantitation. While a quantitation percentage of 45% seems somewhat low, it may have been slightly higher (or lower) if phospholipid isomers were accounted for. However, LIPID MAPS did not include information about which isomers were human in origin, which were found in mammalian species but which would be expected to be found in humans and which isomers are known to be either human but not expected to be found in blood or non-human and specific only to other mammals. Therefore, the phospholipid annotation in LIPID MAPS was not sufficient to determine which phospholipid isomers should be included in a list of potentially-detectable human plasma phospholipids. It would therefore be misleading to draw strong conclusions about the method bias based on the calculation of percentage of total phospholipid isomers quantitated without more information.

3.4.4. Multivariate Analysis

In order to show whether there were any differences between the LC/MS profiles from the MetS patients and the healthy controls, *unsupervised* principal component analysis (PCA) was performed as a first step towards distinguishing a separation between the MetS and healthy control groups, without providing the program with any grouping information about the samples analyzed. However, it was found that the two groups could not be well distinguished, probably due to the large degree of biological variability in humans. Next, PLS-DA was employed as a *supervised* multivariate analysis approach for data modeling to reveal any group separation trends between the MetS and the healthy control groups. In contrast to the unsupervised PCA approach in which no sample group information is provided by the user, this supervised data modeling approach was carried out by providing the software with information about which samples belonged to which group. The PLS-DA data modeling revealed that the R^2 values for data acquired in both positive and negative ion modes are close to 1.00 for the first 3 principal components. These large R^2 values are an indication of good fit to the model, as it is evidence of minimal noise in the data. It also indicates almost all of the distinction between the MetS group and the healthy control (Y) group is explained by the phospholipid peak areas (X). The Q^2 values for data sets acquired in both the positive and negative ion modes are both ≥ 0.5. These

large Q^2 values also provide evidence of minimal noise in the data, while at the same time indicating good predictability of the model. Therefore, the two PLS-DA models generated from both the positive and negative ion modes were able to predict whether new phospholipid profiles would belong to the MetS group or to healthy control group. A large Q^2 is also an indication that the model is not dominated by scattered outliers. In addition, because all of the sample points lie within the ellipse in Figure 13, we can conclude that at the 95% confidence level, no sample outliers were detected. Therefore, using PLS-DA data modeling, based on the LC/MS data, the distinction between the MetS and control groups is well-explained by the phospholipid abundances, and the model has the ability to predict to which sample group a new patient sample would belong.

Because the model was determined to be suitable, the information about the data revealed by the model could be examined. The ability of PLS-DA to detect a visibly-distinct separation between the MetS group and the healthy control group is indicative of a detectable difference between MetS samples and the healthy control samples. Because this difference was detected using imported peak areas from LIPID MAPS-matched phospholipids, we concluded that PLS-DA detected a difference in the MetS group *vs.* healthy control group due solely to differences in plasma *phospholipid* abundances. If these differences can be linked to *specific* phospholipids, we may be able to determine a plasma phospholipid signature of human metabolic syndrome. To investigate into whether this was the case, for each data set (in each ion detection mode), the top 10 phospholipids contributing most to the separation between MetS and healthy control groups were examined. Because an average VIP value should be equal to 1, values larger than 1 are indicative of important X-variables (phospholipids). The VIP values for all top 20 phospholipids are well above 1, indicating that all of these phospholipids are considered important to the separation between the two groups. The large peak area standard deviations associated with some phospholipids can be attributed to the expected high degree of biological variability in humans, which can result from different environmental interactions, such as different lifestyles. Figures 15 and 16 show that 19 of these 20 top phospholipids are found at higher abundances in the MetS group than in the healthy controls. Only 1 of the 20 was found at a lower abundance in the MetS group as compared to healthy controls. From Figure 15 it is visible that in positive ion mode, species corresponding to matched phospholipid neutral masses 493.3168 Da, 495.3325 Da and 523.3638 Da are found at a higher abundance in MetS. The species corresponding to

matched phospholipid mass 817.5985 Da shows decreased abundance in MetS. From Figure 16, in negative ion mode, species corresponding to matched phospholipid masses 767.5101, 805.5622 Da, 815.5465 Da, 829.5622 Da, and 833.5935 Da all show an approximate, increased abundance in MetS ≥ 2-fold. This is very interesting and may point to their potential role in MetS pathogenesis or at least their potential as phospholipid biomarkers for detection of MetS.

3.3.5. Univariate Analysis

Figures 17 and 18 display the distribution of data points for each of the top 20 most significant phospholipids as boxplots. Each box itself displays the 25th to 75th percentile of data (the interquartile range). The vertical line that extends downwards from the bottom of this box represents the bottom 25th percentile of data (including the minimum) while the vertical line extending upwards from the top edge of the box represents the uppermost 75th percentile of data (including the maximum). The spread of the data at various quartiles can be visualized by examining the height of the box as well as the lengths of the vertical lines extending outwards from the box (the range). The medians for all sample groups appear to be approximately centered within the interquartile range for both sample groups for 18 of the top 20 phospholipids. An analysis of the location of the median in relation to the interquartile range allows us to evaluate the skewness of the data. The medians for both sample groups for almost all top 20 significant phospholipids appear to be approximately centered within the interquartile range. Skewness to the left was clear for species 817.5985 Da in positive ion mode and species778.5513 Da in negative ion mode. Some skew to the right was visible for species corresponding to masses 493.3168 Da, 523.3638 Da, and 731.5465 Da and 767.5101. Some skew to the left was visible for species corresponding to 755.5465 Da and 788.5513 Da. Overall, these observations suggest that the data does not appear to be greatly skewed. We can also get an idea for the kurtosis of the data by examining the data spread, or range. The interquartile range is fairly similar for most of the top 20 phospholipids. This meant that, generally, the dispersion between groups was comparable. A total of 6 of these 20 interquartile ranges are visibly different (493.3168 Da, 662.5250 Da, 805.5822 Da, 815.5465 Da, 817.5985 Da and 833.5935 Da). All but two of the tighter distributions in this case belong to the control group. This could point to a biological stressor that impacts the tight regulation of certain phospholipid

species in MetS. Overall, however, the kurtosis of the data does not appear to be very abnormal. Also noteworthy is the fact that there is very little overlap of the interquartile regions for data from almost all top 20 significant phospholipids. This may point to a statistically-significant contribution to the difference between MetS and control groups attributable to this specific phospholipid. It may also be of interest to note that the only outlier detected fell outside the acceptable abundance range of healthy controls, but within the range of the abundance in MetS. This could also provide evidence in support of the hypothesis that MetS is still not well-characterized, and further emphasizes the need for a more specific definition of MetS.

For testing normality with the Ryan-Joiner test, the null hypothesis (h_0) states that data are normally distributed. Minitab reported a general value of "$P > 0.100$" for all values of P greater than 0.100. However, if $P \leq 0.100$, the exact P value associated with this test was reported. At the 95% confidence level, when $P > 0.100$, the null hypothesis could not reasonably be rejected and samples were deemed to have come from normally distributed data. All statistical parameters (averages, variances, standard deviations, degrees of freedom, etc.) were calculated by Minitab for both the MetS group (1) and the healthy control group (2) for all top 20 phospholipids. If samples failed the normality test, a non-parametric test would have been used. However because all phospholipids passed the Ryan-Joiner tests for normality, a parametric test was used. As shown in appendix B, the P values for all Ryan-Joiner tests for normality were greater than 0.100. This meant that we have little reason to conclude that quantitation data was not normally distributed. Data for both MetS groups and healthy controls was concluded to have come from a normally-distributed population.

For Levene's test, the null hypothesis assumes that the variance of the first group is equal to the variance of the second group (h_0: $\sigma_1 = \sigma_2$). Therefore, at a confidence level of 95%, the null hypothesis was rejected if $P \leq 0.05$ and it was concluded that the sample variances were statistically different. Sample variances were concluded to be similar when $P > 0.05$. After the normality and equality of variances for the two sample populations were tested, the two sample means for each of the top 20 significant phospholipids were compared using the appropriate independent, two sample, two-tailed t-test at the 95% confidence level. When statistical proof was sufficient for the rejection of the null hypothesis, sample variances were determined not to be similar and a t-test for unequal variances was conducted in Minitab. When the statistical proof was insufficient to allow for the rejection of the null hypothesis, sample variances were

deemed statistically similar ($P > 0.05$), and a t-test for equal variances was conducted in Minitab. Also, the Levene's test was performed to test equality of variances as this test does not rely on normality. Conducting a Levene's test ensured that results were not dependent on the results of another test. In addition, although not used, Minitab simultaneously generated a P value for both F test and Levene's test for all of the top 20 phospholipids. P values from F tests indicated that for almost all phospholipids, the null hypothesis was rejected at lower values of P and accepted at higher values. This seems to point to Levene's test as being more conservative. A more conservative test is useful for small sample sizes when it can be tempting to make stronger conclusions than appropriate based on limited information. Next, to test for equality of variances, the Levene's test was used. From appendix B, we see that for 8 of the top 20 phospholipids, the P values associated with the Levene's test were < 0.05. This meant that there was insufficient evidence to accept the null hypothesis (h_0: $\sigma_1 = \sigma_2$) at the 95% confidence level. Therefore, the null hypothesis was rejected and for these 8 phospholipids, the variances for the MetS group *vs.* the healthy control group were concluded to be statistically unequal. Because the Levene's test returned P values for the remaining 12 of top 20 phospholipids > 0.05, the null hypothesis was rejected. Therefore, for these phospholipids, the variances for the MetS group *vs.* the healthy control group were statistically concluded to be equal.

The null hypothesis for these t-tests stated that the two sample group means were equal (h_0: $\mu_1 = \mu_2$ or h_0: $(\mu_1 - \mu_2) = 0$). Therefore, if $P \leq 0.05$, the difference between the average peak areas for the MetS group *vs.* that of the healthy controls could not be attributed to random sampling error. In this case, average peak areas were deemed statistically different between MetS and healthy controls. The t-test was chosen to determine whether phospholipid abundances between the two sample groups were significantly different. This is because there was no reason to assume the sample data did not come from a normally-distributed population. Also, non-parametric tests lack statistical power with small sample sizes. In addition a two-tailed t-test was performed rather than a one-tailed t-test, because phospholipid abundance associated with MetS samples *vs.* controls was only suspected to be different, but not specifically increased or decreased, prior to multivariate analysis. An independent, two sample, two-tailed t-test for unequal variances was conducted for the 8 (of the top 20) phospholipids with unequal variances at the 95% confidence level. An independent, two sample, two-tailed t-test for equal variances was conducted on the remaining 12 phospholipids with similar variances at the 95%

confidence level. Again, in table 3, we see that for all t-tests for each of the top 20 phospholipids, $P < 0.05$ and for 17 of the 20 phospholipids, $P \leq 0.01$ which is strong evidence against the null hypothesis. Therefore, the null hypothesis (h_0: $\mu_1 = \mu_2$ or h_0: $(\mu_1-\mu_2) = 0$) was rejected in favour of the alternative hypothesis (h_1: $\mu_1 \neq \mu_2$ or h_1: $(\mu_1-\mu_2) \neq 0$) for all top 20 phospholipids. This meant that the differences in phospholipid abundance between the MetS group and the healthy controls were determined to be statistically significant for all top 20 phospholipids.

3.4.6. Structural Identification by MS/MS and Accurate Mass

While MS/MS experiments were conducted for many of the top 20 phospholipids, a clear MS/MS spectrum could only be acquired for one of these without further optimization. However, all fragmentation ions matched theoretical m/z values within 1.2 ppm. For several phospholipids, the signal intensity of the precursor ion was too weak to observe any product ions upon CID fragmentation. Another reason for the lack of good quality MS/MS spectra for this experiment was that for many species of interest there were other peaks very close in mass to the target m/z value. In this case, to isolate a specific phospholipid ion, a narrower mass window of less than 1 Da had to be used. However, the quadrupole mass filter, as shown in Figure 5 is a low unit-mass resolution mass analyzer. Also, when a narrower mass selection window is used, the intensity of the precursor phospholipid ions dramatically decreases. This would make it difficult to observe any product ions from the precursor ions of the phospholipid of interest. On the other hand, if the mass window was widened one or more minor species were selected and fragmented along with the phospholipid of interest, so that MS/MS spectra were not clean enough to deduce which fragment ions originated from the precursor ion of interest. Therefore, although MS/MS using CID was performed on the FTMS following UPLC fractionation, only one phospholipid (neutral mass = 495.3325 Da) was successfully confirmed using this strategy. In future, improved chromatographic resolution and sample enrichment steps, e.g., using an LC separation orthogonal to the current reversed-phase LC method, could potentially be used to ultimately enhance the MS/MS-based structural confirmation.

3.5.Summary

UPLC/QTOF MS has been employed to detect differences in the human plasma phospholipid profiles in MetS patients *vs.* healthy controls. Using multivariate and univariate statistics, 20 phospholipids were shown to be associated with statistically-significant differences between the MetS patients and the healthy controls. The 5 of these 20 species that could be assigned to unique phospholipid structures are PE(18:1/0:0), PC(16:1/0:0), PC(16:0/0:0), PC(18:3/0:0), and PC(18:0/22:6).

Four of these 5 phospholipids assigned unique phospholipid structures were phosphatidylcholines. Also, 4 of these 5 phospholipids, that could each be assigned a unique structural identity, were found in higher abundances in MetS plasma samples than in plasma samples from normal patients. Interestingly, all 4 of the phospholipids found in higher abundance in MetS contained acyl chains with a very high degree of saturation. This agrees with the results from previously-mentioned studies which found that increased blood levels of fatty acids with a high degree of saturation (especially 16:0, 16:1, 18:1, 18:3) were associated with pathogenic states including MetS.[22-24] In addition, a study that aimed at identifying phospholipids involved in type 2 diabetes suggested that the phospholipid with a molecular mass of 495.3325 Da had potential to be used as a biomarker for type 2 diabetes.[64] In addition, this same study also recommended a phospholipid corresponding to neutral mass 523.3638 Da as a biomarker for type 2 diabetes.[64] This agrees with the findings of this current study in that the species corresponding to matched phospholipid mass of 523.3638 Da was found to be one of the top 20 most significant phospholipids. This is very promising as these 2 species were not the species that exhibited the greatest differences between MetS and control groups. This could point to the biomarker potential of other species in the list of the top 20 most significant phospholipids as determined in this study, especially those found with changes $\geq$ 2-fold in MetS.

The one structurally-identified phospholipid which contained a 22:6 acyl chain (mw of 817.5985 Da) is the phospholipid that was found to be decreased in abundance in MetS. Because this phospholipid is decreased in MetS while the other 4 phospholipids with structures are increased, this phospholipid may have implications for the pathogenesis of MetS. In fact, a recent review provides evidence of strong support for the protective benefits of fatty acid 22:6 (Docosahexaenoic acid, DHA) for the prevention of CVD.[78] DHA has also been shown to

favourably modulate other diseases, such as autoimmune disorders, Crohns disease and cancer.[76] While there is little research correlating the phospholipid head group with disease, aforementioned recent studies have correlated dyslipidemia of specific fatty acids with diseases of the metabolism and/or obesity. The findings of this current study agree with previously-reported increases in saturated and monounsaturated fatty acids in disorders related to metabolism. The prevalence of poly-unsaturated fatty acids in phospholipids that were decreased in MetS also supports pre-existing research. These fatty acids, as mentioned above, appear to have a protective effect on metabolism and have been linked to improved blood lipid profiles as well as decreased risk of obesity. It should be noted that this is the first comprehensive study to identify statistically-significant differences in abundances of specific human plasma phospholipids in metabolic syndrome patients *vs.* healthy controls.

Chapter 4: Conclusions and Future Work

4.1. Experimental Methodology

This study applied both FTICR MS and QTOF MS, in combination with DI and LC, for comprehensive metabolomic analysis of human plasma phospholipids. A high degree of specificity was obtained by the ultrahigh mass accuracy and ultrahigh mass resolution obtainable by FTICR MS. The FTICR MS-derived data allow for the efficient assignments of hundreds of phospholipids based on accurate mass measurements alone. In addition, the use of LIPID MAPS, the large, pre-existing database of experimentally-detected phospholipids was beneficial for the phospholipid-targeted approach to data analysis. This provided assurance that all accurate masses matching phospholipids from the database had already been detected and identified in mammalian tissues. Therefore, the risk of (incorrectly) identifying a theoretical phospholipid that does not exist in nature is reduced. The creation of a final list of identified phospholipids using this method could be beneficial for future targeted studies, as it reduces the risk of species that are not of interest interfering with data interpretation. Phospholipid profiling prior to relative quantitation lays a foundation for further in-depth studies. A preliminary, non-targeted metabolomic analysis can also provide useful information about the sample to facilitate selection of potential targets for further, targeted analysis.

The high sensitivity of mass spectrometry allowed quantitative analysis of samples with limited volume. As demonstrated by this study, using only 25 μL of each human plasma sample, a successful quantitative analysis of hundreds of phospholipids can be performed. The most powerful component of the method developed for this study was arguably the mass-directed approach to data extraction. Using a previously-generated mass list, containing only the species to be studied, added a great deal of specificity to the analysis and facilitates confident data interpretation. Phospholipid-directed data extraction reduces the risk of incorrectly attributing the effects of non-phospholipid species to phospholipids. This promotes correct data interpretation, and eliminates reliance on software parameters that may not be well understood.

The use of multivariate statistics *via* data modeling for detecting quantitative differences in MetS *vs.* healthy groups confirms that individuals with MetS can be distinguished from

healthy individuals based solely on their plasma phospholipid profiles. By conducting multivariate analyses of all of the phospholipids identified, the most important phospholipid species can be pinpointed and selected for further targeted analyses. In this study, the most important phospholipids were selected for identification by MS/MS and for univariate analysis. Subjecting specific phospholipid species to univariate statistics is necessary to gain insight into the mechanism of disease inferred by the phospholipids found to have statistically-significant differences in abundance between MetS and controls. Univariate statistics provides an additional level of confidence in the conclusions made based on results. The methods developed for use in this study should prove useful for the analysis of metabolites from a variety of biological samples as well as for the study of other metabolic disorders.

4.2.New Findings

4.2.1. Human Plasma Phospholipid Profiling

The phospholipid profiling experiment involved in this study assigned a large number of phospholipids based on the high mass accuracy achieved by FTICR MS. In this way, a total of 488 masses matched phospholipid masses when querying the LIPID MAPS database, with a maximum mass error of 6 ppm. Approximately 65% of these masses had associated mass errors below 3 ppm. Among these assigned phospholipids, PC, PE and PS were determined to be the most abundant classes in human plasma, and the least abundant lipid classes in human plasma were found to be SM and CerP. As far as we know, this number (488) represents one of the largest numbers of phospholipids detected in human plasma in a single experiment.

4.2.2. Quantitation of Human Plasma Phospholipids in MetS *vs.* Controls

Multivariate analysis showed a clear separation between the MetS group and the healthy control group based on these phospholipid entities. This means that the human plasma phospholipid profile in individuals with MetS is statistically different from that of the healthy controls, showing a significant difference in the abundance of human plasma phospholipids in MetS patients as compared to healthy controls. A total of 5 phospholipids contributing the most to this difference in phospholipid abundance between MetS and healthy controls were assigned

to unique structural entities in the LIPID MAPS database. Univariate analyses confirmed the statistically-significant differences (at a confidence level of 95%) in the plasma concentrations of all of the top 20 significant phospholipids, including the 5 phospholipids that could be assigned a structural identity. To the best of our knowledge, this is the first study to demonstrate quantitative differences in human plasma phospholipids in MetS patients *vs.* healthy controls, and the results have revealed a potential plasma phospholipid signature of human metabolic syndrome.

4.3.Limitations

It should be noted that approximately 72% of the 488 phospholipid masses were associated with phospholipid isomers in the LIPID MAPS database. Without further structural differentiation between the isomers of these phospholipid species, it is very difficult to make a confident statement concerning the exact number of different phospholipids within each phospholipid class.

Although there are appreciable advantages of the methodology used for this study, it is important to recognize that there are several drawbacks as well. Using a pre-existing database to identify compounds has several limitations. In doing so, potentially-important species may be excluded from further analyses if they are not already present in the database. In addition, LIPID MAPS contains lipids found in mammals including, but not limited to, humans. This implies possible incorrect assignments of phospholipids unique to non-human mammalian species as being human. Ideally, accurate mass measurements should be used in conjunction with MS/MS experiments to confirm the structural identities of these phospholipids, especially for the identification of the positions of the double-bonds in the fatty acid tail regions. In this way, the molecular mass, retention time, and MS/MS spectrum can be combined in a complementary manner to confirm the complete structural identity of the phospholipids. However, due to the low abundance of many of these phospholipids in complex plasma samples, a significant amount of research into MS/MS method optimization may be necessary, as well as the development of possible sample enrichment techniques. However, this type of structural analysis would provide a more confident structural assignment.

A limitation of LC/MS for the relative metabolomic quantitation in this study is the difficulty in comparing the results obtained from the positive ion mode analyses with those from the negative ion mode. In addition, phospholipid abundances for various species within a sample cannot be compared without the use of absolute quantitation. This is because the ionization efficiencies and the ionization suppression effects will be different between the two ionization modes as well as between phospholipids. To address this limitation, isotopically-labelled standards could be used as internal standards in order to define absolute concentration values. These concentrations could then be used to compare different analytes within an ionization mode as well as across ionization modes. To prepare isotopically-labelled standards, however, the structural identity of unknown phospholipids must first be determined.

Another limitation of using QTOF MS for the quantitation portion of this study is the decreased mass accuracy of this instrument in comparison to FTICR MS. Because of this, the mass error window for peak integration used was 50 ppm, which meant that the quantitated masses could only be differentiated if two masses differed by > 25 ppm. This meant that the specificity of the LC/FTICR MS, which could differentiate masses differing only by > 6 ppm in the LC/MS analyses, was lost in transferring the method to the QTOF mass spectrometer. Therefore, this contributed to the fact that the true value of 488 phospholipid masses could not be fully realized during quantitation. In addition, during quantitation, this made it difficult to confidently determine which peaks corresponded to which exact masses (for those masses that are separated by a mass difference < 25 ppm).

Also, sample volumes for some of the samples were limited, so only one replicate of the QTOF MS quantitation experiment by QTOF MS could be performed. Ideally, this experiment should be performed in triplicate. In addition, the conclusions based on the findings from this quantitative study must be somewhat tempered by the fact that the cohort size was very small and contained only 18 individuals. In addition, as with any study using human samples, diet and environmental interaction cannot be entirely controlled. For these reasons, a large amount of biological variability can be expected. The age, gender and ethnicity of study subjects could have been matched between the two groups to control some of this. However, the aim of this study was to determine whether the phospholipid profile of MetS could be distinguished from healthy controls in general. In addition, the statistical tests used on this data were selected based on their suitability for small sample sizes as well as statistical power – and these tests did

confirm the presence of MetS-related differences even without controlling for this human variablity.

4.4. Future Work

There are a few key recommendations for follow-up studies to the current study. First, the results observed could be validated with a larger sample cohort. Also, more comprehensive data processing and analysis should be performed to eventually include all metabolite features detected in human plasma, if improved data processing approaches can be found. In this way, potentially-important metabolites, especially those not included in any currently available metabolome databases could be measured and would not go undetected. This would be very important for the discovery of potential metabolite biomarkers of any disease, including metabolic syndrome.

Further studies could also be conducted to expand the current work and achieve a better understanding of MetS. If possible, the phospholipid differences of three distinct sample groups could be studied: individuals who meet MetS criteria, lean healthy controls, and obese individuals who do not meet MetS criteria. This would aid in distinguishing general obesity from MetS, which is not always clearly distinguished in literature.

Bioinformatic techniques for the study of phospholipid differences between MetS and healthy controls could also be employed if detailed information about the abundance of specific plasma phospholipid species was monitored. Ideally, a long-term (*e.g.,* 10 year) follow-up study could be conducted to correlate phospholipid irregularities with individuals who later develop either T2DM and/or CVD. In this way, it could be determined whether specific phospholipids are associated more strongly with onset of disease, and, more interestingly, whether certain phospholipids are specific risk factors for CVD or are specific risk factors for T2DM. These specific phospholipids could also be correlated with increased risk of premature mortality so that certain phospholipids could be used to predict increased disease morbidity. If these studies prove successful, plasma phospholipids associated with MetS could add a substantial amount of diagnostic power to MetS as a predictor of T2DM, CVD, and mortality.

References

1. "IDF Worldwide Definition of the Metabolic Syndrome. International Diabetes Federation IDF." *International Diabetes Federation IDF*. Web. 6 July 2010. http://www.idf.org/metabolic_syndrome.

2. Reaven, G. M. "Banting lecture 1988. Role of insulin resistance in human disease." *Diabetes* 37.12 (1988): 1595-1607.

3. Alberti, K. et al. "Harmonizing the Metabolic Syndrome." *Circulation* 120.16 (2009):1640-5.

4. Anand, S.S. et al. "Relationship of metabolic syndrome and fibrinolytic dysfunction to cardiovascular disease." *Circulation* 108 **(**2003): 420-5.

5. Dunstan, D. W. et al. "The rising prevalence of diabetes and impaired glucose tolerance." *Diabetes Care* 25.5 (2002):829-34.

6. Alberti, K., Zimmet P. and J. Shaw. "Metabolic syndrome—a new world-wide definition. A Consensus Statement from the International Diabetes Federation." *Diabetic Medicine* 23.5 (2006):469-480.

7. Pischon, T. et al. "General and abdominal adiposity and risk of death in Europe." *The New England Journal of Medicine* 359.20 (2008):2105-20.

8. Andreassi, M. G. "Metabolic syndrome, diabetes and atherosclerosis: influence of gene-environment interaction." *Mutation Research* 667.1-2 (2009):35-43.

9. Ferguson, J. F. et al. "Gene-nutrient interactions in the metabolic syndrome: single nucleotide polymorphisms in ADIPOQ and ADIPOR1 interact with plasma saturated fatty acids to modulate insulin resistance." *The American Journal of Clinical Nutrition* 91.3 (2010):794-801.

10. Adamo, K. et al. "Gene-environment interaction and the metabolic syndrome." *Novartis Foundation Symposium* 293(2008):103-19.

11. Ordovas, J. and J. Shen. "Gene-environment interactions and susceptibility to metabolic syndrome and other chronic diseases." *Journal of Periodontology* 79.8 Suppl (2008):1508-13.

12. Hossain, P., Kawar B. and M. El Nahas. "Obesity and diabetes in the developing world--a growing challenge." *The New England Journal of Medicine* 356.3 (2007):213-5.

13. Dawson, K. G. et al. "The economic cost of diabetes in Canada, 1998." *Diabetes Care* 25.8 (2002):1303-7.

14. Turner, R. C. et al. "Risk factors for coronary artery disease in non-insulin dependent diabetes mellitus: United Kingdom Prospective Diabetes Study (UKPDS: 23)." *British Medical Journal; International Edition* 316.7134 (1998):823-8.

15. Tarride, Jean-Eric, et al. "A review of the cost of cardiovascular disease." *The Canadian Journal of Cardiology* 25.6 (2009):e195-202.

16. "Health Canada Economic Burden of Illness in Canada in 1998 Ottawa" *Health Canada*; 2002. Web. 6 July 2010. http://www.phac-aspc.gc.ca/publicat/ebic-femc98

17. Thom, T. et al. "Heart disease and stroke statistics--2006 update: a report from the American Heart Association Statistics Committee and Stroke Statistics Subcommittee." *Circulation* 113.6 (2006):e85-151.

18. "Cardiovascular Diseases." *World Health Organization WHO*. Web. 6 July 2010. http://www.who.int/cardiovascular_diseases/en.

19. "Dyslipidemia - Medical Definition and More from Merriam-Webster." *Dictionary and Thesaurus - Merriam-Webster Online*. Web. 10 April 2011. http://www.merriam-webster.com/medical/dyslipidemia.

20. Krauss, R. M. et al. "AHA Dietary Guidelines: revision 2000: A statement for healthcare professionals from the Nutrition Committee of the American Heart Association." *Stroke* 31.11 (2000):2751-66.

21. Nagao, K. and T. Yanagita. "Bioactive lipids in metabolic syndrome." *Progress in Lipid Research* 47.2 (2008):127-46.

22. Warensjö, E., Riserus U. and B. Vessby. "Fatty acid composition of serum lipids predicts the development of the metabolic syndrome in men." *Diabetologia* 48.10 (2005):1999-2005.

23. Aguilera, C., Gil-Campos M. and R. Canete. "Alterations in plasma and tissue lipids associated with obesity and metabolic syndrome." *Clinical Science* 114(2008):183-93.

24. Warensjo, E. et al. "Factor analysis of fatty acids in serum lipids as a measure of dietary fat quality in relation to the metabolic syndrome in men." *The American Journal of Clinical Nutrition* 84.2 (2006):442-8.

25. Yanagita, T. and K. Nagao. "Functional lipids and the prevention of the metabolic syndrome." *Asia Pacific Journal of Clinical Nutrition* 17.S1 (2008):189-91.

26. Merritt, J. C. "Metabolic syndrome: soybean foods and serum lipids." *Journal of the National Medical Association* 96.8 (2004):1032-41.

27. Shirouchi, B et al. "Effect of dietary omega 3 phosphatidylcholine on obesity-related disorders in obese Otsuka Long-Evans Tokushima fatty rats." *Journal of Agricultural and Food Chemistry* 55.17 (2007):7170-6.

28. Huang, T. et al. "Plasma phospholipids n-3 polyunsaturated fatty acid is associated with metabolic syndrome." *Molecular Nutrition & Food Research*.

29. Hergenc, Gulay et al. "Serum Total and High-Density Lipoprotein Phospholipid Levels in a Population-Based Study and Relationship to Risk of Metabolic Syndrome and Coronary Disease." *Angiology* 59 (March 2008): 26-35.

30. Lehninger, A. L. "Principles of biochemistry." New York (1993).

31. Spiegel, S. and A.H. Merrill Jr. "Sphingolipid metabolism and cell growth regulation." *The FASEB Journal* 10.12 (1996):1388-97.

32. Cui, Z. and M. Houweling. "Phosphatidylcholine and cell death." *Biochimica et Biophysica Acta*. 1585.2-3 (2002):87-96.

33. Polichetti, E. et al. "Dietary polyenylphosphatidylcholine decreases cholesterolemia in hypercholesterolemic rabbits: Role of the hepato-biliary axis." *Life Sciences* 67.21 (2000):2563-76.

34. Jiang, Y., Noh S. K. and S. I. Koo. "Egg phosphatidylcholine decreases the lymphatic absorption of cholesterol in rats." *The Journal of Nutrition* 131.9 (2001):2358-63.

35. Buang, Y. et al. "Dietary phosphatidylcholine alleviates fatty liver induced by orotic acid." *Nutrition* 21.7-8 (2005):867-73.

36. Stamler, C. J. et al. "Phosphatidylinositol promotes cholesterol transport in vivo." *Journal of Lipid Research* 41.8 (2000):1214-21.

37. Burgess, J. W. et al. "Phosphatidylinositol increases HDL-C levels in humans." *Journal of Lipid Research* 46.2 (2005):350-5.

38. Murata, M., Imaizumi K. and M. Sugano. "Effect of dietary phospholipids and their constituent bases on serum lipids and apolipoproteins in rats." *The Journal of Nutrition* 112.9 (1982):1805-8.

39. Imaizumi, K. et al. "The contrasting effect of dietary phosphatidylethanolamine and phosphatidylcholine on serum lipoproteins and liver lipids in rats." *The Journal of Nutrition* 113.12 (1983):2403-11.

40. Nikolic, M. et al. "Efflux of cholesterol and phospholipids derived from the haemoglobin-lipid adduct in human red blood cells into plasma." *Clinical Biochemistry* 40.5-6 (2007):305-9.

41. Jauhiainen, M et al. "Human plasma phospholipid transfer protein causes high density lipoprotein conversion." *The Journal of Biological Chemistry* 268.6 (1993):4032-6.

42. Dettmer, K., Aronov P. A. and B. D. Hammock. "Mass spectrometry-based metabolomics." *Mass Spectrometry Reviews* 26.1 (2007):51-78.

43. Gu, H. et al. "Principal component directed partial least squares analysis for combining nuclear magnetic resonance and mass spectrometry data in metabolomics: application to the detection of breast cancer." *Analytica Chimica Acta* 686.1-2 (2011):57-63.

44. Pan, Z. and D. Raftery. "Comparing and combining NMR spectroscopy and mass spectrometry in metabolomics." *Analytical and Bioanalytical Chemistry* 387.2 (2007):525-7.

45. van der Greef, J. and A. K. Smilde. "Symbiosis of chemometrics and metabolomics: past, present, and future." *Journal of Chemometrics* 19.5-7 (2005):376-86.

46. Fenn, J. B. et al. "Electrospray ionization for mass spectrometry of large biomolecules." *Science* 246.4926 (1989):64-71.

47. Kozlowski, R. L., Shah, B. and Borchers C. H. (in-press). Emerging mass spectrometry-based technologies for the analysis of chromatin changes. *Methods in molecular biology*.

48. Guilhaus, M. "Special feature: Tutorial. Principles and instrumentation in time-of-flight mass spectrometry. Physical and instrumental concepts." *Journal of Mass Spectrometry* 30.11 (1995):1519-32.

49. Mamyrin, B A. "Time-of-flight mass spectrometry (concepts, achievements, and prospects)." *International Journal of Mass Spectrometry* 206.3 (2001):251-66.

50. Wollnik, H. "Time-of-flight mass analyzers." *Mass Spectrometry Reviews* 12.2 (1993):89-114.

51. Miller, P. E. and M. B. Denton. "The quadrupole mass filter: Basic operating concepts." *Journal of Chemical Education* 63.7 (1986):617-23.

52. Dawson, P. H. "Quadrupole mass analyzers: Performance, design and some recent applications." *Mass Spectrometry Reviews* 5.1 (1986):1-37.

53. Koppenaal, D. W. et al. "MS detectors." *Analytical Chemistry* 77.21 (2005):418A-427A.

54. Harris, F. M. et al. "Signal-to-noise ratios in the measurement of low ion currents using electron multipliers." *Mass Spectrometry Reviews* 3.2 (1984):209-29.

55. Marshall, A. G., Lin Wang T. C. and T. Lebatuan Ricca. "Ion cyclotron resonance excitation/de-excitation: A basis for Stochastic fourier transform ion cyclotron mass spectrometry." *Chemical Physics Letters* 105.2 (1984):233-36.

56. Marshall, A. G. and C. L. Hendrickson. "Fourier transform ion cyclotron resonance detection: principles and experimental configurations." *International Journal of Mass Spectrometry* 215.1-3 (2002):59-75.

57. Amster, I. J. "Fourier transform mass spectrometry." *Journal of Mass Spectrometry* 31.12 (1996):1325-1337.

58. "About the consortium: Nature Lipidomics Gateway." *Home: Nature Lipidomics Gateway*. Web. 22 July 2010. http://www.lipidmaps.org/aboutconsortium.html.

59. Sud, M. et al. "LMSD: lipid maps structure database." *Nucleic Acids Research* 35.Database issue (2007):D527-32.

60. "Databases: Nature Lipidomics Gateway." *Home: Nature Lipidomics Gateway*. Web. 22 July 2010. http://www.lipidmaps.org/data/structure/index.html.

61. Wiseman, J. M. et al. "Mass spectrometric profiling of intact biological tissue by using desorption electrospray ionization." *Angewandte Chemie*. International Edition in English 44.43 (2005):7094-7.

62. Kim, J. Y. et al. "Metabolic profiling of plasma in overweight/obese and lean men using ultra performance liquid chromatography and Q-TOF mass spectrometry (UPLC-Q-TOF MS)." *Journal of Proteome Research* 9.9 (2010):4368-75.

63. Want, E. J. et al. "Ultra performance liquid chromatography-mass spectrometry profiling of bile acid metabolites in biofluids: application to experimental toxicology studies." *Analytical Chemistry* 82.12 (2010):5282-9.

64. Wang, C. et al. "Plasma phospholipid metabolic profiling and biomarkers of type 2 diabetes mellitus based on high-performance liquid chromatography/electrospray mass spectrometry and multivariate statistical analysis." *Analytical chemistry* 77.13 (2005):4108-16.

65. Niwa, T. et al. "Increased glutathionyl hemoglobin in diabetes mellitus and hyperlipidemia demonstrated by liquid chromatography/electrospray ionization-mass spectrometry." *Clinical Chemistry* 46.1 (2000):82-8.

66. Pepys, M. B. et al. "Targeting C-reactive protein for the treatment of cardiovascular disease." *Nature* 440.7088 (2006):1217-21.

67. Bligh, E. G. and W. J. Dyer. "A rapid method of total lipid extraction and purification." *Canadian Journal of Physiology and Pharmacology* 37.8 (1959):911-17.

68. Bao, Y. et al. "Effect of repeated freeze-thaw cycles on urinary albumin-to-creatinine ratio." *Scandinavian Journal of Clinical & Laboratory Investigation* 69.8 (2009):886-8.

69. Murias, M., Rachtan M. and J. Jodynis-Liebert. "Effect of multiple freeze-thaw cycles of cytoplasm samples on the activity of antioxidant enzymes." *Journal of Pharmacological and Toxicological Methods* 52.2 (2005):302-5.

70. Reynolds, B. et al. "Effect of repeated freeze-thaw cycles on routine plasma biochemical constituents in canine plasma." *Veterinary Clinical Pathology* 35.3 (2006):339-40.

71. Han, J. et al. "Towards high-throughput metabolomics using ultrahigh-field Fourier transform ion cyclotron resonance mass spectrometry." *Metabolomics* 4.2 (2008):128-40.

72. Cuyckens, F. and M. Claeys. "Optimization of a liquid chromatography method based on simultaneous electrospray ionization mass spectrometric and ultraviolet photodiode array detection for analysis of flavonoid glycosides." *Rapid Communications in Mass Spectrometry* 16.24 (2002):2341-8.

73. Eichholtz, T. et al. "The bioactive phospholipid lysophosphatidic acid is released from activated platelets." *Journal of Biochemistry* 291.3 (1993):7631-4.

74. Fellmann, P. et al. "Transmembrane Movement of Diether Phospholipids in Human Erythrocytes and Human Fibroblasts." *Biochemistry* 39.17 (2000):4994-5003.

75. Bomalaski, J. S. et al. "Uptake of fatty acids and their mobilization from phospholipids in cultured monocyte-macrophages from rheumatoid arthritis patients." *Clinical Immunology and Immunopathology* 39.2 (1986):198-212.

76. Wang, C. et al. "Identification of phospholipid structures in human blood by direct-injection quadrupole-linear ion-trap mass spectrometry." *Rapid Communications in Mass Spectrometry* 19.17 (2005):2443-53.

77. Pang, L. Q. et al. "Simultaneous determination and quantification of seven major phospholipid classes in human blood using normal-phase liquid chromatography coupled with electrospray mass spectrometry and the application in diabetes nephropathy." *Journal of Chromatography A* 869.1-2 (2008):118-25.

78. Connor, W. E. "Importance of n-3 fatty acids in health and disease." *The American Journal of Clinical Nutrition* 71.1 (2000):171S-5S.

Appendix

Appendix A. Database-Matched Phospholipid Masses Detected by FTICR MS.
Table listing all 488 LIPID MAPS-matched phospholipid masses as detected by DI and LC coupled to FTICR MS. Each phospholipid accurate mass is displayed alongside its corresponding mass error (ppm).

Molecular Mass	Mass Error (ppm)	Molecular Mass	Mass Error (ppm)	Molecular Mass	Mass Error (ppm)	Molecular Mass	Mass Error (ppm)	Molecular Mass	Mass Error (ppm)	Molecular Mass	Mass Error (ppm)
368.1964	3.26	486.2746	2.88	521.3481	0.38	550.3998	5.63	596.2962	3.35	645.5097	0.46
396.2277	2.27	493.3168	0.00	523.2910	4.40	551.3223	4.90	598.3118	3.18	646.5050	0.46
421.2593	1.66	493.3532	3.45	523.3638	0.19	553.3380	3.80	600.3275	3.83	647.5254	0.93
422.2433	4.26	494.3372	1.01	525.2855	0.19	565.3744	3.89	606.4624	3.46	654.3744	4.89
432.2277	3.24	495.3325	0.61	529.3168	2.46	566.3584	4.06	607.4213	3.29	654.4624	3.21
436.2590	5.50	498.2958	1.61	533.3845	0.94	567.3172	0.00	609.3642	2.63	656.4781	5.18
437.2906	2.52	499.2699	1.20	535.4002	2.05	567.3325	0.88	614.3431	0.33	657.4370	3.65
450.3110	1.11	501.2855	0.00	536.3478	5.22	567.3536	1.06	616.4104	2.11	658.4937	0.76
451.2699	3.10	503.3012	0.60	537.3794	0.19	569.2754	0.88	617.4057	2.75	662.4887	1.21
453.2855	2.65	507.3325	0.20	538.3271	5.57	571.3638	0.70	617.4784	0.16	662.5250	0.75
464.3379	2.80	507.3689	0.00	539.3223	2.78	572.2962	2.80	620.2962	1.29	664.4104	4.36
465.3219	1.50	508.2801	3.74	541.3168	0.18	576.4155	3.82	620.4781	2.10	666.4836	5.10
467.3012	0.00	509.3481	0.00	542.2492	2.03	578.3948	5.53	622.4210	0.64	672.4730	3.72
475.2699	2.52	509.3845	2.16	543.3325	1.66	578.4311	5.53	630.4624	1.74	673.5410	0.59
477.2855	0.21	510.2958	3.14	545.2754	1.83	579.3900	5.70	631.4213	5.86	674.4887	0.00
479.3012	0.21	511.2910	3.13	545.3481	4.03	581.3693	3.10	634.4937	0.79	674.5250	5.04
479.3376	0.21	511.3274	1.37	547.2910	1.64	586.3635	3.24	635.4526	4.72	675.5567	2.81
481.3168	0.21	512.3114	1.37	547.3638	0.18	588.3791	2.38	638.2469	1.10	677.4996	0.30
481.3532	0.00	517.3168	0.58	549.3067	1.09	593.4057	3.71	638.3948	5.64	677.5359	1.18
484.2801	2.06	519.3325	0.39	549.3794	0.18	595.3485	0.84	643.4941	0.31	678.4261	5.90

Molecular Mass	Mass Error (ppm)	Molecular Mass	Mass Error (ppm)	Molecular Mass	Mass Error (ppm)	Molecular Mass	Mass Error (ppm)	Molecular Mass	Mass Error (ppm)	Molecular Mass	Mass Error (ppm)
678.4472	5.90	704.5832	2.27	723.5203	1.52	741.5309	1.75	749.5359	0.13	759.5414	1.45
678.4624	2.36	705.5309	0.43	723.5567	1.24	741.5672	1.35	750.5200	2.93	759.5778	0.13
679.4213	2.06	708.4730	0.99	724.5043	0.41	743.5465	0.67	750.5411	0.40	760.5618	1.58
680.4781	2.94	708.4941	1.55	725.5359	0.69	743.5829	0.67	750.5775	4.66	762.5563	0.00
682.4937	3.52	710.5250	5.49	726.5200	3.44	744.4730	5.10	751.5152	1.86	763.5152	2.62
684.3850	4.82	712.5407	5.61	727.5516	2.06	745.5622	0.40	751.5516	0.80	763.5363	0.00
684.5094	2.63	713.4996	3.92	728.4628	2.61	745.5985	1.21	752.4992	5.71	763.5727	1.96
690.5563	1.16	715.5152	1.40	728.5832	0.96	746.4887	0.27	752.5356	5.85	764.5356	1.31
691.5516	0.72	715.5516	4.19	729.5309	0.82	746.5462	4.29	753.5309	3.72	764.5720	0.65
692.4417	5.20	717.4581	2.23	729.5672	3.15	746.5826	3.62	753.5672	1.19	765.5309	0.65
698.4006	0.86	717.5309	0.56	729.6036	2.33	746.6189	2.54	755.5465	1.32	765.5672	1.96
698.4887	1.43	717.5672	0.56	730.5989	0.14	747.5050	0.80	755.6193	0.79	766.4785	4.83
699.5203	0.43	718.5513	3.34	731.5465	0.27	747.5203	1.34	756.5669	2.78	766.5876	0.13
700.5407	0.71	719.5465	0.14	731.5829	3.28	747.5414	2.81	757.5258	1.58	767.5101	4.82
701.5359	2.00	719.5829	0.97	732.3251	0.55	747.5778	2.01	757.5622	1.72	767.5465	0.26
701.5723	4.28	720.4730	0.28	732.6145	2.05	747.6142	4.68	757.5985	0.53	767.5829	0.13
702.5676	0.85	720.5305	0.28	733.5622	0.68	748.5043	2.54	757.6349	1.58	769.5258	1.04
703.5152	0.14	721.4894	5.68	734.5462	3.40	748.5254	0.80	758.5462	5.54	769.5622	3.12
704.4628	5.68	722.3408	2.08	736.5618	2.04	748.5618	1.07	758.6189	1.71	769.5985	0.78
704.5720	3.55	722.4887	0.55	739.5152	2.03	749.5207	5.07	758.6302	2.77	771.5414	2.98

Molecular Mass	Mass Error (ppm)	Molecular Mass	Mass Error (ppm)	Molecular Mass	Mass Error (ppm)	Molecular Mass	Mass Error (ppm)	Molecular Mass	Mass Error (ppm)	Molecular Mass	Mass Error (ppm)
771.5778	0.39	779.5829	1.41	789.5309	0.63	794.5826	3.78	803.6040	5.35	809.6298	3.58
771.6142	3.50	780.5669	2.82	789.5520	2.91	795.5414	2.51	804.5153	5.10	811.5363	4.93
772.5618	3.49	781.5622	1.02	789.5672	5.57	795.5778	3.77	804.5880	1.99	811.6091	0.37
772.6346	1.81	781.5985	3.84	789.5884	1.65	795.6142	0.63	804.6244	0.87	812.5567	5.91
773.5571	0.00	783.5050	1.28	790.5724	3.04	797.5207	3.39	805.5622	1.86	812.5931	1.97
773.5935	0.52	783.5778	1.91	790.6088	2.02	797.5935	0.13	805.5833	0.87	812.6771	0.00
773.6298	2.71	783.6142	1.53	791.5101	3.28	797.6298	1.76	805.5985	5.34	813.5520	2.46
774.5200	0.52	784.5254	4.84	791.5465	0.13	799.5363	4.38	805.6197	5.46	813.6248	0.98
774.6139	5.81	784.5982	3.57	791.5676	3.28	799.6091	0.00	806.5309	3.60	814.6928	0.49
775.5363	3.09	785.5571	2.55	791.5829	2.27	799.6455	1.00	806.5462	1.12	815.5465	1.59
775.5516	3.61	785.5935	1.78	791.6040	1.39	801.5309	5.36	806.5826	1.36	815.5676	3.07
775.5727	4.00	785.6298	0.25	792.4730	3.03	801.5520	2.62	806.6037	1.98	815.6404	0.98
776.5567	0.52	786.5775	4.58	792.4789	4.42	801.5884	4.99	806.6401	5.70	816.4789	1.96
776.5931	5.92	786.6615	2.92	792.5153	3.41	801.6248	1.00	807.5050	1.24	816.6608	0.24
777.5520	0.64	787.5363	2.03	792.5880	1.89	801.6611	1.50	807.5778	1.86	816.7084	0.61
777.5672	3.34	787.5727	1.14	792.6244	2.78	802.5513	4.24	808.5102	4.08	817.5622	2.32
778.5149	5.91	787.6091	2.41	793.5258	3.65	802.5724	2.12	808.5618	1.73	817.5833	0.49
778.5513	3.21	787.6455	0.63	793.5622	2.90	803.5465	5.35	808.6458	2.72	817.5985	0.61
778.5724	0.00	788.6295	0.38	793.5985	0.13	803.5676	0.62	809.5207	0.49	817.6197	2.69
779.5465	5.00	788.6771	0.89	794.5309	5.41	803.5829	5.23	809.5935	1.48	817.6561	4.65

Molecular Mass	Mass Error (ppm)	Molecular Mass	Mass Error (ppm)	Molecular Mass	Mass Error (ppm)	Molecular Mass	Mass Error (ppm)	Molecular Mass	Mass Error (ppm)	Molecular Mass	Mass Error (ppm)	Molecular Mass	Mass Error (ppm)
818.4945	4.52	827.5676	0.24	835.5363	0.24	848.5415	4.48	859.6666	4.65	878.5884	0.91	912.5728	0.66
818.6037	5.13	827.6040	3.50	835.6091	0.48	848.5567	0.24	860.5415	4.53	880.5102	5.56	918.5235	2.94
819.5414	0.12	828.5880	3.86	836.5415	1.08	849.5520	3.18	861.6248	0.46	880.6041	2.27	924.6092	4.87
819.5778	1.59	829.5622	4.22	836.5779	5.86	849.6611	0.82	862.5571	1.62	881.6146	0.45	930.5599	4.19
819.5989	2.44	829.5833	0.48	837.5520	3.46	850.5571	4.23	862.6663	2.78	882.5258	0.23	940.5442	2.66
819.6142	0.61	830.6037	5.54	837.6248	0.36	851.5676	0.59	863.6404	0.35	884.5415	5.54	946.5912	4.86
819.6353	5.25	831.5778	2.89	838.5935	0.60	851.6040	3.88	864.6092	4.63	886.5571	0.34	976.5078	1.84
820.5102	5.85	831.5989	0.60	839.5465	1.31	851.6768	0.00	865.5833	1.39	887.5676	5.30	978.5235	4.80
820.5466	4.75	831.6353	5.05	839.5676	3.69	852.5728	1.64	866.4945	0.92	888.5728	3.38		
820.6193	2.07	831.6717	0.12	839.6404	4.64	852.5880	1.99	868.5466	5.30	888.6819	3.04		
821.5935	0.49	832.5466	3.36	841.5833	1.54	852.6092	0.12	870.5258	1.72	890.4922	2.58		
821.6298	1.58	832.6193	4.80	841.6561	3.09	853.5833	0.47	870.5411	4.02	890.6976	1.35		
823.5363	2.91	832.6557	4.56	842.6401	4.87	853.6924	3.05	872.6506	4.47	892.5102	1.12		
823.6091	2.91	833.5207	1.80	843.5989	2.02	855.5989	0.35	873.7187	4.58	894.5258	0.22		
823.6455	0.24	833.5935	1.44	845.6146	2.72	855.6353	3.39	874.5724	2.40	894.5622	1.68		
824.5567	4.97	833.6146	0.60	845.6298	0.35	857.5935	1.63	875.6615	4.34	896.5415	3.12		
825.5520	0.73	833.6510	0.60	845.7237	1.30	857.6146	0.12	876.5728	1.83	901.7500	2.33		
825.5884	1.33	834.5258	3.48	846.5622	3.66	858.5258	3.03	876.6819	0.57	903.6928	4.20		
825.6611	0.97	834.5622	0.96	846.6350	4.96	859.5363	5.24	877.5622	0.68	908.6354	5.17		
826.5724	4.23	834.5775	5.27	847.6455	0.47	859.6302	3.96	877.5833	2.05	910.5571	0.00		

Appendix B. Test Statistics for Univariate Analysis of Top 20 Phospholipids.
Statistical-test values calculated by Minitab are displayed in the table below for all top 20 phospholipids (as determined by multivariate analysis). Statistical test values calculated using a t-test for unequal variances are marked with an asterisk. Otherwise, a t-test for equal variances was conducted.

Test Statistic	467.3012	479.3012	493.3168	495.3325	517.3168	523.3638	662.5250	674.5250	720.5305	731.5465
Two-Tailed T-test Statistic	3.28*	3.68*	3.86*	3.50	3.14	3.19	3.79	3.64	4.39	2.93
T-test Degrees Freedom	11	11	11	16	16	16	16	16	16	16
T-test P-value	0.007	0.004	0.003	0.003	0.006	0.006	0.002	0.002	0.000	0.010
Levenes Test P-value	0.002	0.004	0.003	0.366	0.470	0.164	0.080	0.080	0.060	0.127
Ryan-Joiner Test P-value	> 0.100	> 0.100	> 0.100	> 0.100	> 0.100	> 0.100	> 0.100	> 0.100	> 0.100	> 0.100

Test Statistic	753.5309	755.5465	767.5101	777.5520	778.5513	805.5622	815.5465	817.5985	829.5622	833.5935
Two-Tailed T-test Statistic	2.89	2.87	3.55	4.56*	5.30	3.56*	4.02*	-2.97	3.24*	3.06*
T-test Degrees Freedom	16	16	16	10	16	8	9	16	9	8
T-test P-value	0.011	0.011	0.003	0.001	0.000	0.007	0.003	0.009	0.010	0.016
Levenes Test P-value	0.186	0.396	0.203	0.034	0.351	0.004	0.012	0.102	0.018	0.006
Ryan-Joiner Test P-value	> 0.100	> 0.100	> 0.100	> 0.100	> 0.100	> 0.100	> 0.100	> 0.100	> 0.100	> 0.100